2015-01-01

Carbon Based Nano-Composite Materials For Energy Storage Applications

Gerardo Rodriguez Melo
University of Texas at El Paso, gerardorodriguez1990@gmail.com

CARBON BASED NANO-COMPOSITE MATERIALS FOR ENERGY STORAGE APPLICATIONS

GERARDO RODRIGUEZ MELO

Department of Mechanical Engineering

APPROVED:

Yirong Lin, Ph.D., Chair

Juan C. Noveron, Ph.D.

Binata Joddar, Ph.D.

Charles Ambler, Ph.D.
Dean of the Graduate School

CARBON BASED NANO-COMPOSITE MATERIALS FOR ENERGY STORAGE APPLICATIONS

by

GERARDO RODRIGUEZ MELO, Bachelor of Science in Mechanical Engineering

THESIS

Presented to the Faculty of the Graduate School of

The University of Texas at El Paso

in Partial Fulfillment

of the Requirements

for the Degree of

MASTER OF SCIENCE

Department of Mechanical Engineering

THE UNIVERSITY OF TEXAS AT EL PASO

August 2015

Abstract

Energy storage systems and devices are an integral part of advanced electronic technology. Electronic technology is ever-advancing, but in order to do so, it must be supported by all its systems. The energy storage system is one key system that may dictate the performance and limitation of such electronics. Thus, research emphasis on energy storage devices has been on improving the performance of energy storage devices, such as: improved energy and power density, increased stability and cycle life, as well as reduced costs. Lithium-ion-batteries, and supercapacitors offer the potential to meet energy storage demands and to be improved further upon. Herein, novel hybrid electrode materials utilizing high surface area carbon structures and transition metal oxide nanomaterial are implemented to improve the energy storage performance in lithium-ion-battery and supercapacitor applications. Initial characterization methods for all the electrode materials include: scanning electron microscopy (SEM), transmission electron microscopy (TEM), and x-ray diffraction (XRD). Supercapacitor performance is improved by utilizing porous-carbon/cerium-oxide nanoparticle (PC-CON) hybrid electrode material synthesized via a low temperature hydrothermal method and using tretraethyl ammonium tetrafluroborate in acetonitrile as the organic electrolyte. This electrode material allows for a hybrid capacitance mechanism that utilizes both, electric-double-layer capacitance and pseudocapacitance. Additionally, the excellent electrode-electrolyte interaction due to the electronchemical properties of the ionic electrolyte provides a better voltage window. Electrochemical measurements performed using a potentio-galvanostat revealed that the specific capacitance was improved by 30% using PC-CON electrode material compared with pure porous carbon. Lithium-ion-battery performance is improved over porous carbon by implementing two different hybrid anode materials: one utilizing porous-carbon/cerium-oxide nanoparticles (PC-CON) and the other utilizing microwave-reduced (exfoliated) graphene-oxide/titanium-oxide nanowires (MEGO-TON). High surface area carbon structures such as porous carbon and microwave-reduced graphene oxide alone provide high lithiation and excellent cycling capability

by shortening the transport length for Li^+ ions with the large electrode/ electrolyte interface. Addition of a transition metal oxide structure such as cerium oxide nanoparticles, which offer a high redox potential, can enhance surface electrochemical reactivity and increase capacity retention capability for a higher number of cycles, while the addition of titanium oxide nanowires, which offer high specific surface area, serve to improve lithium-ion electrode/electrolyte intercalation. Battery performance was measured using a battery analyzer. It was determined that the PC-CON hybrid anode material showed significantly higher specific capacity and better capacity retention, while the MEGO-TON hybrid showed even better results with a specific capacity improvement of 80% over porous carbon, as well as an improved charge-discharge rate.

Table of Contents

List of Figures

Chapter 1: Introduction

1.1 Energy Storage

As a whole, an energy storage system is any kind system that is capable of storing or accumulating energy of any type or form so that it may be delivered at a convenient time to do useful work. Energy can be stored in several forms, these include: chemical, gravitational potential energy, electrical potential, kinetic energy, elastic energy, etc. Herein, the energy storage systems and devices being discussed pertain mainly to the storage of electrical potential energy and electrochemical energy. Therefore, the main focus and perspective of this thesis is in respect with such energy storage devices.

1.2 Motivation of Research

The motivation of this research is to support the development of energy storage devices, which are often integrated into complex electrical systems. The aim of this research is to investigate and improve upon existing energy storage devices, particularly supercapacitors and lithium-ion batteries—with a focus on the anode materials implemented. By improving the performance of these energy storage devices, the development of ever advancing electronic technology is also supported.

Modern technology is heavily inclined toward electronic devices; this delves into considerations such as their design, materials used, applications, evolution, etc. The current typical trend (advancement) for most, if not all, electronic devices is to generally make them cheaper, smaller, lighter weight, more responsive, and more reliable. The goal of this trend aims to produce electronic devices with higher performance and capabilities than ever before. Electronic devices are usually made up of several integrated systems and components. One of the key systems that

must be up-to-par in order to extract the most performance out of any electronic device, is its energy storage system(s)—which is also responsible for delivering that stored energy. Consequently, energy storage and delivery systems are also evolving in order to keep up with the overall advancement of electronic technology. This means that research everywhere is being conducted with the purpose of improving the energy and power density, efficiency, stability and service life of energy storage devices.

The broader scale for the motivation of this research in energy storage devices deals with the greater world-wide issues that we presently face. It has been documented and it is clear that the demand for energy throughout the world is ever increasing (see Figure 1). Developed countries around the world have created everyday needs for oil and electricity, and thus have created a high demands for this type of energy in order to maintain their technological infrastructure.

Today, most of our energy comes from the burning of non-renewable fossil fuels; primarily coal, oil, and natural gas (Figure 2 and 3). Due to high energy demands and requirements, there is an energy stream that trickles all the way down from fossil fuels, to the power plants and power grids, all the way down to some of these energy storage devices—typically found in portable electronics. Thus, a performance increase in energy storage devices may have a cumulative impact on a bigger overall scale too.

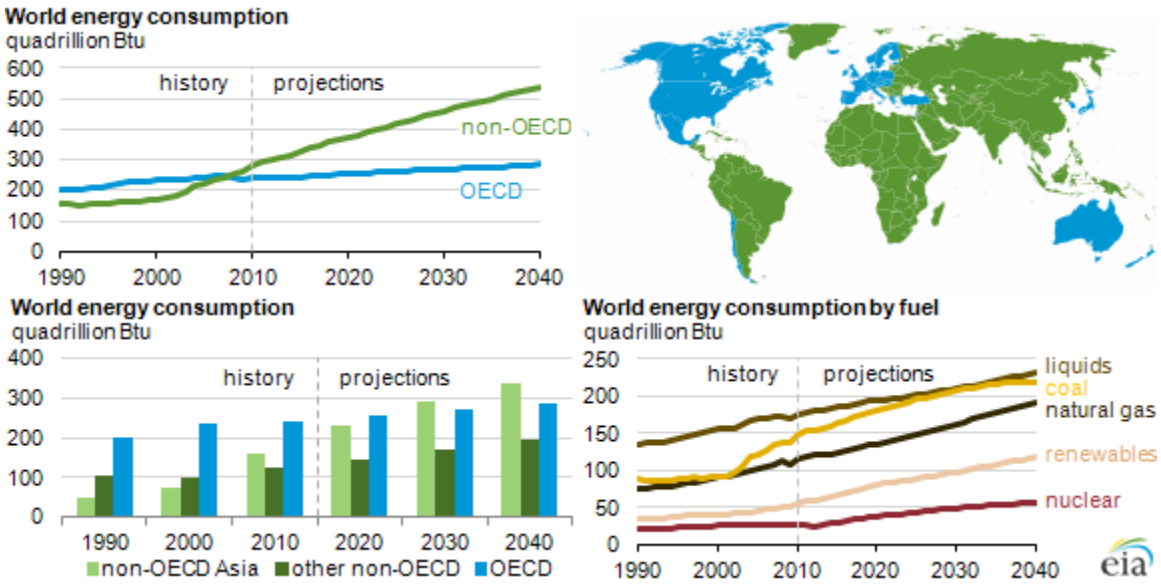

Figure 1. Projected world energy consumption [1].

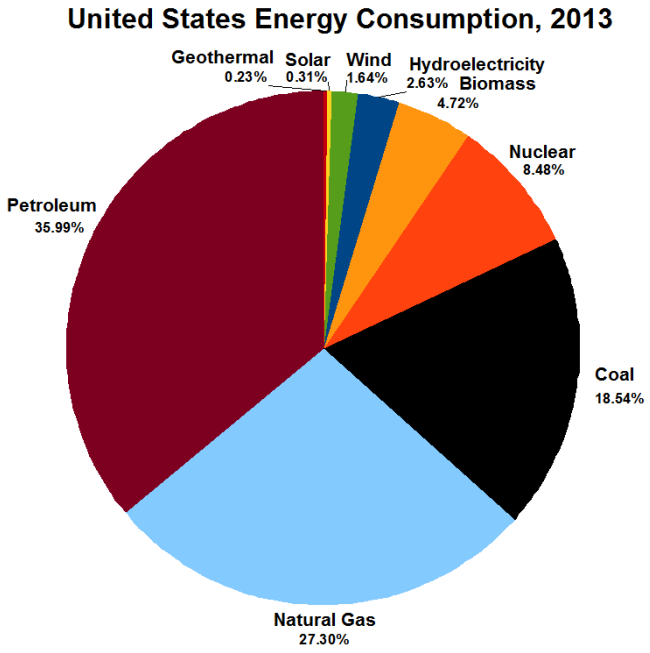

Figure 2. United States Energy Consumption, 2013 [2].

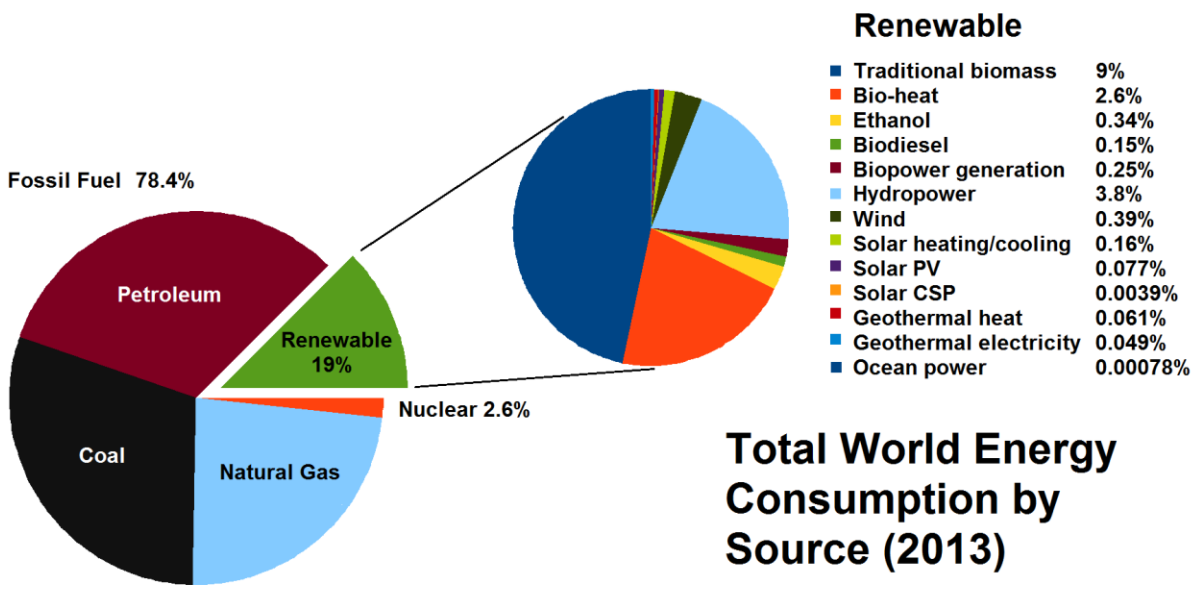

Figure 3. Total World Energy Consumption by Source, 2013 [3].

Chapter 2: Background

2.1 Graphene

2.1.1 Introduction to Graphene

Graphene is one of the many physical forms (allotropes) of elemental carbon. It is a planar monolayer of carbon atoms arranged into a tightly packed two-dimensional honeycomb lattice, and it is the basic building block for graphitic materials of all other dimensions (as can be seen on Fig. 4). Graphene can adsorb and desorb various atoms and molecules, thus creating an existence of graphitic derivatives [4]. The particular structure of graphene contributes to its particular and extraordinary characteristics. Electrons in graphene behave like massless relativistic particles which contribute to graphene's peculiar properties such as an anomalous quantum Hall effect and the absence of (electron) localization [5]. Additionally, the structure of graphene gives it phenomenal mechanical, electrical and thermal properties as well as other interesting properties (such as the quantum Hall effect) that are outside the scope of this thesis. Electrically, graphene is more conductive than any other substance known, its mechanical strength is 200 times greater than that of steel at a sixth of the weight, and its thermal conductivity is greater than that of diamond [6].

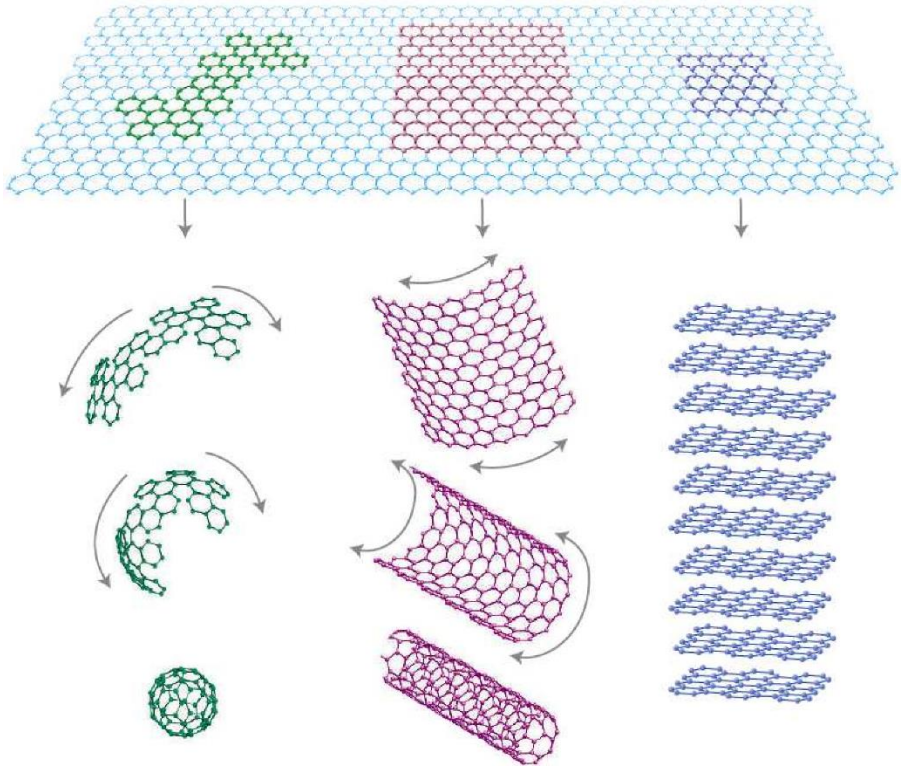

Figure 4. Graphene—building block of other graphitic material: graphite, carbon nanotubes, fullerenes [7].

What constitutes graphene as a true 2-dimensional material? It has been shown through research that the electronic structure of graphene rapidly evolves with the number of layers, thus, this criterion would establish a 3-dimensional limit of 10 layers, by which then, graphene would be considered a thin graphite film [7]. Only graphene, and to a good approximation, its bilayer has simple electronic spectra: they are both zero-gap semiconductors (they can also be referred to as zero-overlap semimetals) with one type of electron and one type of hole [7]. For three or more layers, the spectra become increasingly complicated: several charge carriers appear, and the conduction and valence bands start to notably overlap [7].

2.1.2 Properties

Graphene's properties and stability is due to a tightly packed, periodic array of carbon atoms and an sp^2 orbital hybridization: a combination of orbitals p_x and p_y that constitute the σ-bond [8]. Graphene has three σ-bonds and one π-bond. The final p_z electron makes up the π-bond, and is key to the half-filled band that permits free-moving electrons [8]. It has been said that electrons in SLG behave as massless relativistic particles (relativistic, in the sense that the particles must be moving close to or at the speed of light and thus theoretically not experience time) [4-7]. The sigma bonding arrangement acting within a single graphene layer is extremely strong; the individual graphene layer is probably the toughest two-dimensional network structure known, and it is the structural backbone of all carbon/graphite fibers, and carbon nano-tubes [8]. Figure 5 shows a conceptual image of carbon's atomic structure and its hybridization of bonds when forming a single layer of carbon atoms or graphene. This in-plane toughness results from the strong covalent sigma (σ) bonds that hold carbon atoms in the graphene layers together [8]. This high in-plane strength is the basis of all carbon fibers and carbon nanotubes [8]. Each carbon atom in a graphene layer has three sigma atomic orbitals, which combine with similar orbitals of neighboring carbon atoms, creating the molecular bonds that hold the layer together. The stiff sigma bonds that give rigidity and high tensile strength to a graphene layer do not provide any support in the perpendicular direction [8].

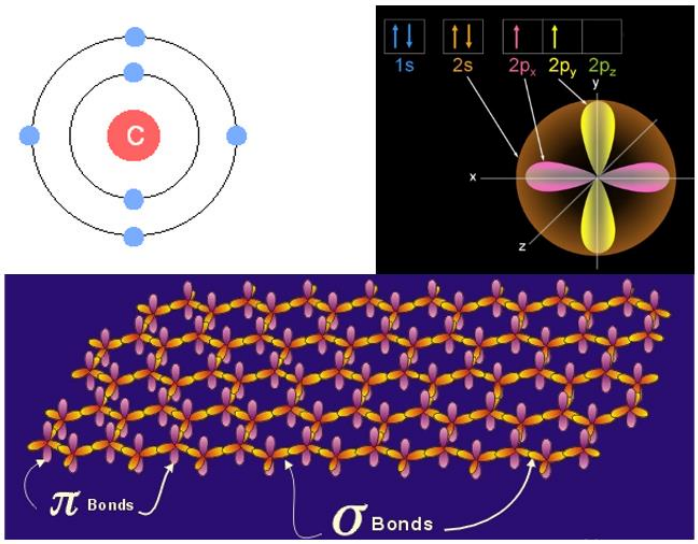

Figure 5. Carbon's atomic structure, orbitals (top images), and orbital hybridization to form a single graphene layer (bottom image) [8-10].

The pi component is the result of weak, secondary electrical bonds formed by the overlapping pi (p) orbitals of the sp2 carbon network within each graphene sheet; each carbon atom has one pi electron—this electron has a high probability of being found in a region just above or below the plane formed by the carbon atoms in a graphene layer [8]. Each graphene layer can be visualized as a system of fused six-carbon rings, one can also visualize that superimposed above and below each ring there exists a ring or donut shaped region, containing six pi electrons (one from each carbon atom) [8]. These pi electrons are not stationary, but are "de-localized" within the confines of the donut shaped region they occupy—this delocalization is "conjugated" throughout the contiguous graphene layer; this means that there is some mechanism for pi electrons to be delocalized not only in their immediate orbital, but to move back and forth between and within adjacent orbitals [8]. Thus, electrons in graphene behave like massless relativistic particles which contribute to graphene's peculiar properties such as an anomalous quantum Hall effect and the absence of (electron) localization [4,5,7].

The investigation of pristine graphene has brought about incredible property discoveries. An extremely high charge mobility of 230,000 cm2/Vs has been reported [5]. Graphene's charge carriers exhibit giant intrinsic mobility, have zero effective mass, and can travel for micrometers without scattering (at room temperature); graphene can sustain current densities six orders of magnitude higher than that of copper [4]. Estimated experimental thermal conductivity of single-layer (pure defect free) graphene is a record high of ~3000 W/mK to ~5000 W/mK [5]. After carbon nanotubes, graphene has been reported to have the highest elastic modulus and strength [5]. Researchers have determined the intrinsic mechanical properties of single, bilayer, and multiple layers of graphene. A single, defect free graphene layer is predicted to show the highest intrinsic tensile strength: E~1 TPa, and σ~130 GPa [5]. Due to these amazing properties, pristine graphene has obtained a great deal of attention, especially for its conducting capabilities which give graphene great potential in electronics and heat-dissipation applications. However, the low yield production of pristine graphene makes it unfeasible for large yield and budget production of practical graphitic derived components. Graphene oxide (GO) can be produced in relatively large quantities at a lower cost, while its properties still showing potential for practical applications especially upon reduction, which produces reduce graphene oxide (RGO). As fabricated, GO is found to be insulating due to the presence of oxidized functional groups [5]. The controlled reduction (thermal or chemical) process results in the removal of oxidized groups causing GO to regain most of its electrical conductivity, however, not all of the oxidized groups will be removed and the remaining groups will still limit the electron transport properties of RGO. Depending on the level of reduction, the conductivity of RGO can vary from 0.05 to 500 S/cm [5].

2.1.3 Fabrication

Currently there are numerous and diverse synthesizing methods for graphene fabrication. The more standard and widely implemented methods include: (Mechanical) Exfoliation and Cleavage, Thermal Chemical Vapor Deposition (CVD) Techniques, and Chemical Exfoliation methods (seen on Fig. 6).

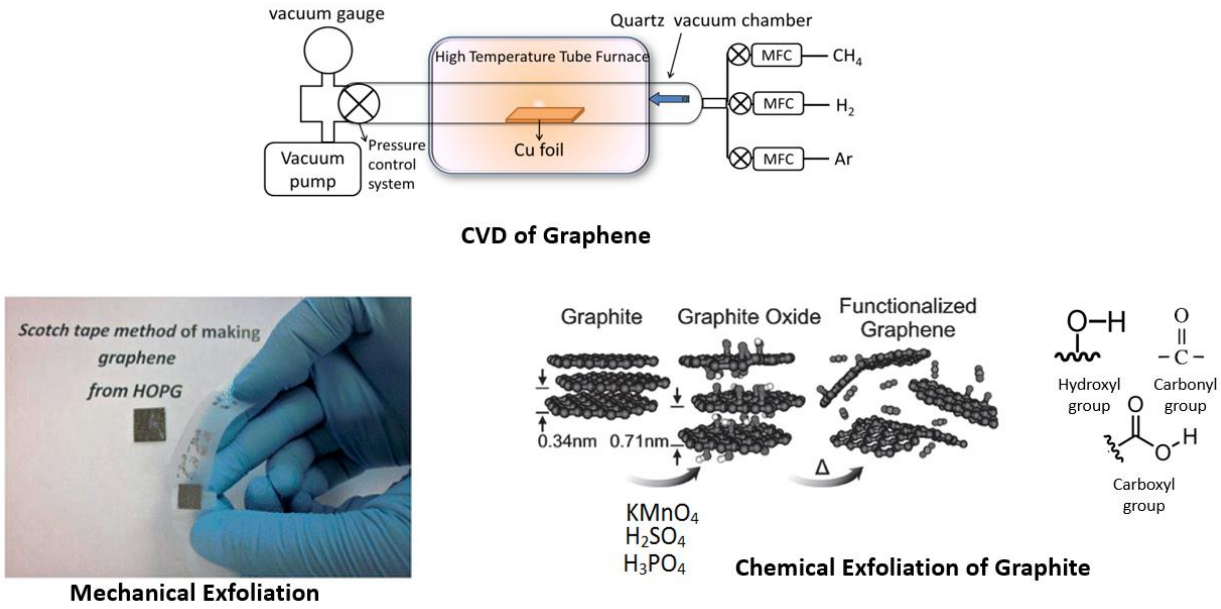

Figure 6. Fabrication methods of graphene [11].

In 2004, Novoselov et al. was accredited with the discovery of graphene; proving that single sheets of carbon are thermodynamically stable and can exist [11]. Novoselov et al. were the first to effectively exfoliate graphite through micro-mechanical cleavage, widely known as the "Scotch-tape" method, which results in the facile production of high-quality graphene crystallites; thus, leading to the explosion of scientific experiments and advancements regarding graphene [11]. Since then, researchers have found many ways to fabricate graphitic material. As just mentioned, few, and single-layer transferable graphene nanosheets were first obtained by mechanical

exfoliation ("Scotch-tape" method) of bulk graphite, and by epitaxial chemical vapor deposition [12]. Chemical vapor deposition (CVD) using copper as the substrate is one of the fastest developing processes to produce single layer graphene due to the low solubility of carbon in copper which leads to a self-limited process. It has been shown that large area growth and excellent device properties can be achieved by this method. The approaches mentioned are preferred for the high quality graphene produced, but yield very small amounts. Chemical means of synthesis/fabrication provide the ability for bulk-scale production of graphene materials. The goal of this research is to further advance the status of graphene a feasible engineering material and expand its utilization for practical applications. Thus a chemical fabrication approach that can yield higher amounts of graphene is preferred here. A chemical approach to graphite exfoliation uses strong oxidizing agents to yield graphene oxide (GO), a nonconductive hydrophilic carbon material; upon reduction, GO can be transformed back into a conductive graphitic material. The chemical approach usually followed is the *Improved Hummer's method* (probably the most common method used today) developed by Marcano et al [12].

Improved Hummer's Method

The improved Hummer's method is implemented for this research, so this sub-section will give a more detailed insight regarding this process.

Advantages of the improved method are a higher yield, a simpler fabrication procedure, no toxic gas evolution during preparation, and equivalent conductivity upon reduction [12]. Once reduced, the graphene oxide resembles a black powder. This form will allow the authors to utilize the graphene for the production of graphene based composites.

Due to the high, ever-increasing, and ever-improving demand for technological energy systems, a graphene fabrication method that favorably suits wide commercialization is desired. Chemical exfoliation methods allow the chemical conversion of bulk graphite into considerable quantities of graphene oxide [5]. Graphene oxide is typically synthesized through the oxidation of graphite using oxidants including concentrated sulfuric acid, nitric acid and potassium permanganate based on the Hummers method [5]. In chemical exfoliation, graphite is chemically intercalated such that graphene planes become separated by layers of intervening atoms or molecules (oxide functional groups in the case of graphene oxide) [7]. The improved method by Marcano et al. allows for fewer defects in the basal plane compared to graphene oxide prepared by the Hummer's method; it also has the advantage of consisting of a simpler protocol, higher yield, no toxic gas evolution during preparation and equivalent conductivity upon reduction [12]. Thus the "Improved Synthesis of Graphene Oxide" method is favored.

Currently, Hummer's method ($KMnO_4$, $NaNO_3$, and H_2SO_4) is widely used for preparing graphene oxide. The improved method excludes the $NaNO_3$, increased the amount of $KMnO_4$, and uses a 9:1 mixture of H_2SO_4/H_3PO_4 to improve the efficiency of the oxidation process [12].

Graphene derived sheets in graphite oxide (graphene oxide sheets) are heavily oxygenated, bearing hydroxyl and epoxide functional groups on their basal plane, in addition to carbonyl and carboxyl groups located at the sheet edges. The presence of these functional groups makes graphene oxide sheets strongly hydrophilic, which allows graphite oxide to readily swell and disperse in water [12].

2.1.4 Applications

As previously stated, the mechanical exfoliation of graphene is not suitable for large scale production, while chemical oxidation of graphite into graphite oxide offers an easy path to obtain

graphene oxide in large quantities that can be reduced chemically, electrochemically or thermally into graphene [5]. The bulk production of GO and RGO thus allows research to be conducted on graphene based composites. Graphene shows promise in the use as filler for polymer matrix composites. Its reinforcement can offer exceptional properties in composites and applications in the fields of electronics, aerospace, automotive, and green energy [5]. Graphene aids in the increase of mechanical properties of a composite, due to the effective load transfer between graphene and polymer, however the most appealing property enhancements that graphene contributes to composites is the increase of electrical and thermal conductivity in otherwise insulating polymer matrix materials. When used as fillers in an insulating polymer matrix material, graphene may greatly enhance the electrical conductivity of the composite; these composite materials can be used for electromagnetic shielding, photovoltaic devices, sensors, and conducting paint [5]. The use of graphene to increase a polymer composite's thermal conductivity may open the opportunity of that composite for applications in electronic circuit boards, heat sinks, and light weight high performance thermal management systems [5]. Despite graphene's amazing thermal conductivity, the thermal conductivity increase of graphene composites is not as high as that of the electrical conductivity increase; typically an increase of the thermal conductivity is of the order of 4, whereas the increase in electrical conductivity is in the order of 15-19 [5]. Overall, the increase in mechanical, thermal, and electrical properties that graphene gives to composites allows for potential graphene composite applications in high-strength, light-weight structural polymer composites for automobile, aerospace, and thermally conductive support in the electronic industry for thermal management, as well as applications of graphene/polymer composites in energy storage, electrically conductive polymers, antistatic coatings and electromagnetic interference shielding [5].

Probably the biggest challenge in graphene composites is the effective and even dispersion of graphene. Graphene tends to agglomerate in solvents and composites mainly due to the strong van der Waals forces. Agglomeration is a problem because as the graphene clumps up with itself, it begins to lose its special properties that separate it from graphite. To counter this, researchers have used a wide range of solvents using a stabilizing polymer [6,13].

2.2 Supercapacitors

2.2.1 Introduction to Supercapacitors

Supercapacitors bridge the significant performance gap between regular capacitors and batteries, as can be seen in Figure 7. While capacitors have a high power density, they possess low energy density. The opposite is the case for batteries—they possess high energy density, but low power density. This means that capacitors can deliver energy quickly, but they don't store much of it, and as for batteries, they can store a large amount of energy in comparison, but they cannot deliver it quickly. Thus, these two energy storage devices are suited for different performance requirement applications.

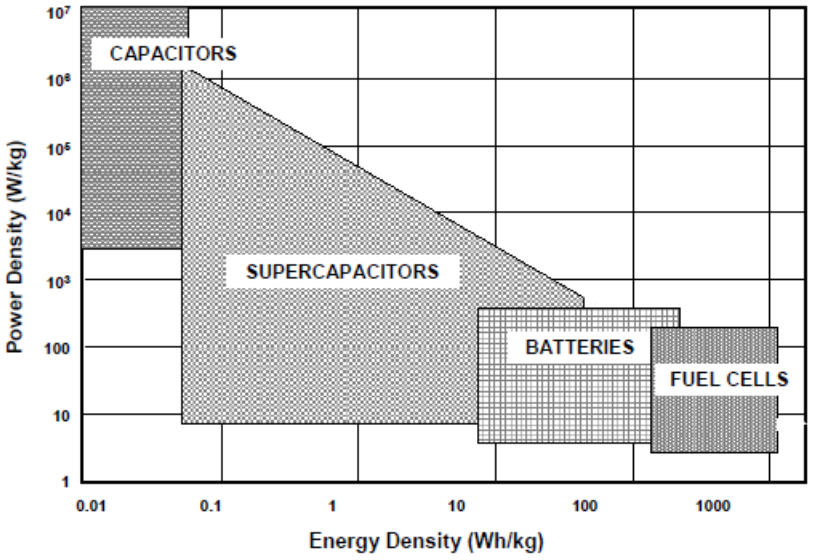

Figure 7. Ragone plot of energy storage devices [21].

Working Principles and Relationships

Supercapacitors, also known as ultracapacitors or electrochemical capacitors, are governed by the same fundamental equations as conventional capacitors, but utilize higher surface area electrodes and thinner dielectrics to achieve greater capacitances. This allows for energy densities greater than those of conventional capacitors and power densities greater than those of batteries. This is why supercapacitors may become an attractive power solution for an increasing number of applications [21].

In order to better understand the fundamental working principles in a supercapacitor, the fundamentals of a simple dielectric capacitor should be explored. A dielectric capacitor is an energy storage device of simple construction. It is typically composed of two parallel plates and a dielectric medium in between the plates; its unit of measure is capacitance equal to 1 Farad per

meter (F/m). There are several relationships that characterize and are characterized by the definition of capacitance. Capacitance (C) is the ability of a material to store an electrical charge. In a parallel plate dielectric capacitor, capacitance can be described as the amount of charge (Q) stored in the parallel plates with respect to the existing voltage (V) between those plates.

$$C = Q/V$$

Capacitance (C) is directly proportional to the area (A) of the parallel plates (or electrodes), and inversely proportional to the distance (D) between the electrodes:

$$C = \varepsilon_0 \varepsilon_r \frac{A}{D}$$

where ε_0, is the permittivity of free space (vacuum) and it is a physical constant approximately equal to 8.854×10^{-12} Farads per meter (F/m). The relative permittivity is represented by ε_r, which is the factor by which the electric field between the charges is decreased or increased relative to vacuum, thus it is also the ratio of the capacitance of a capacitor using a dielectric medium versus a similar capacitor that has free space only between the plates. The relative permittivity (ε_r) is also commonly known as the dielectric constant (k), especially in the field of engineering.

Energy will be stored in the capacitor when a voltage is applied between the two parallel plates, causing a separation of charges which is responsible for a net build-up of charges on both plates; resulting in a positively charged plate and a negatively charged plate whose charges now have the capability to do work once they are discharged. The energy stored in a capacitor can be described by the following relationship:

$$E = \frac{1}{2} C V^2$$

Supercapacitors utilize high surface area electrode materials and thin electrolytic dielectrics to achieve capacitances several orders of magnitude larger than conventional capacitors,

in doing so, supercapacitors are able to attain greater energy densities while still maintaining the characteristic high power density of conventional capacitors [21]. Thus, from the equations described above, this leads to an increase in both capacitance and energy.

For a conventional capacitor: The internal components of the capacitor (e.g., current collectors, electrodes, and dielectric material) also contribute to the resistance, which is measured in aggregate by a quantity known as the equivalent series resistance (ESR). The voltage during discharge is determined by these resistances. When measured at matched impedance (R = ESR), the maximum power P_{max} for a capacitor is given by [21]:

$$P_{max} = \frac{V^2}{4 \times ESR}$$

This relationship shows how the ESR can limit the maximum power of a capacitor [21]. Furthermore, by maintaining the low ESR characteristic of conventional capacitors, supercapacitors also are able to achieve comparable power densities [21]. Additionally, supercapacitors have several advantages over electrochemical batteries and fuel cells, including higher power density, shorter charging times, and longer cycle life and shelf life [21]. Based upon current research and development trends, supercapacitors can be divided into three general classes: electrochemical double-layer capacitors, pseudocapacitors, and hybrid capacitors; each class is characterized by its unique mechanism for storing charge [21]. These are, respectively, non-Faradaic, Faradaic, and a combination of the two [21]. Faradaic processes, such as oxidation-reduction reactions, involve the transfer of charge between electrode and electrolyte. A non-Faradaic mechanism, by contrast, does not use a chemical mechanism, rather, charges are distributed on surfaces by physical processes that do not involve the making or breaking of chemical bonds [21].

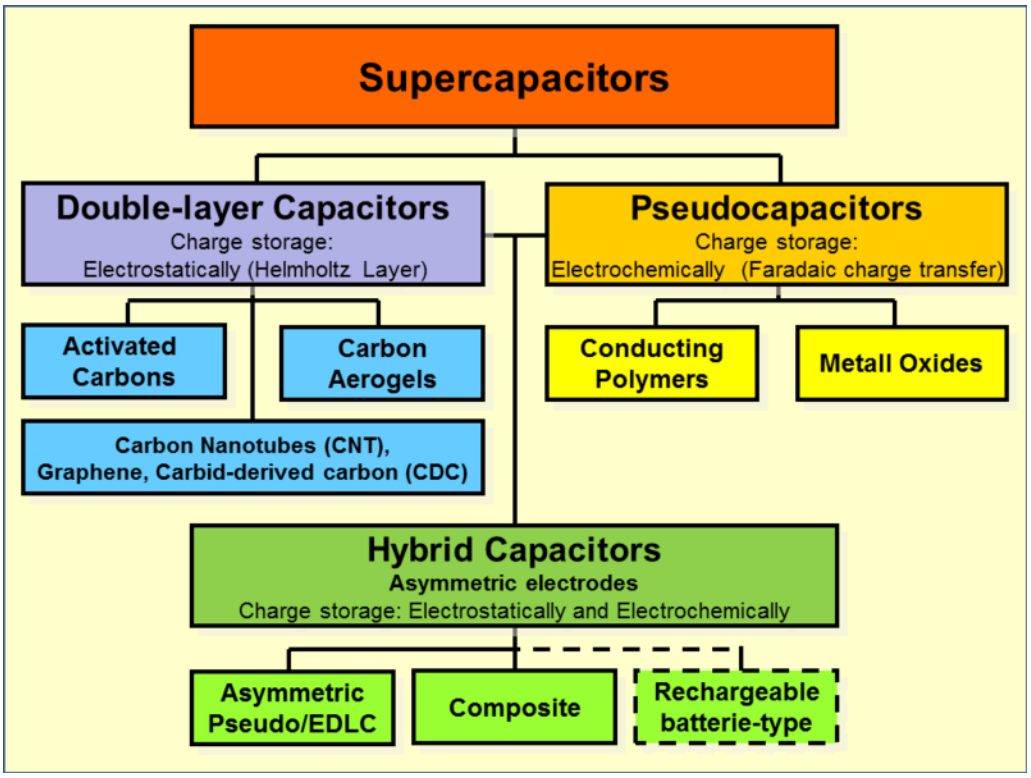

Figure 8. Family tree of supercapacitor types. Double-layer capacitors and pseudocapacitors as well as hybrid capacitors are defined over their electrode designs [17].

Supercapacitors do not have a conventional solid dielectric, they use electrostatic double-layer capacitance or electrochemical pseudocapacitance or a combination of both instead [15, 21, 23]. Electrostatic double-layer capacitors use carbon derivative electrodes with much higher electrostatic double-layer capacitance than electrochemical pseudocapacitance, achieving separation of charge in a Helmholtz double layer at the interface between the surface of a conductive electrode and an electrolyte. The separation of charge is of the order of a few ångströms (0.3–0.8 nm), much smaller than in a conventional capacitor [21]. Electrochemical pseudocapacitors use metal oxide or conducting polymer electrodes with a high amount of electrochemical pseudocapacitance. The typical materials used in order to support the specific supercapacitor mechanism can be seen in Figure 8. Pseudocapacitance is achieved by Faradaic electron charge-transfer with redox reactions, intercalation or electrosorption [21].

Hybrid capacitors, such as the lithium-ion capacitor, use electrodes with differing characteristics: one exhibiting mostly electrostatic capacitance and the other mostly electrochemical capacitance [21].

Storage principles

Electrochemical capacitors use the double-layer effect to store electric energy, however, this double-layer has no conventional solid dielectric which separates the charges. There are two storage principles in the electric double-layer of the electrodes that contribute to the total capacitance of an electrochemical capacitor [14].

- Double-layer capacitance: uses electrostatic storage of the electrical energy achieved by separation of charge in a Helmholtz double layer [21].
- Pseudocapacitance: uses electrochemical storage of the electrical energy achieved by faradaic redox reactions with charge-transfer [15].

Both capacitances are only separable by measurement techniques. The amount of charge stored per unit voltage in an electrochemical capacitor is primarily a function of the electrode size, although the amount of capacitance of each storage principle can vary extremely [18, 21].

Electrode Materials

As before mentioned, the properties of supercapacitors come from the interaction of their internal materials. Especially, the combination of electrode material and type of electrolyte determine the functionality and thermal and electrical characteristics of the capacitors.

As described above, electrical energy is stored in supercapacitors via two storage principles: static double-layer capacitance and electrochemical pseudocapacitance; and the

distribution of the two types of capacitance depends on the material and structure of the electrodes. There are three types of supercapacitors based on storage principle [15, 21]:

- Double-layer capacitors (EDLCs): use activated carbon electrodes or derivatives with much higher electrostatic double-layer capacitance than electrochemical pseudocapacitance [15, 21].
- Pseudocapacitors: use transition metal oxide or conducting polymer electrodes with a high electrochemical pseudocapacitance [15, 21].
- Hybrid capacitors: use asymmetric electrodes, one of which exhibits mostly electrostatic and the other mostly electrochemical capacitance, such as lithium-ion capacitors [15, 21].

Electrolytes

Electrolytes comprise of a solvent and dissolved chemicals that dissociate into positive cations and negative anions, essentially making the electrolyte electrically conductive. The more ions the electrolyte contains, the better its conductivity [17]. In supercapacitors, electrolytes are the electrically conductive medium between the two electrodes. In supercapacitors, the electrolyte provides the molecules for the separating monolayer in the Helmholtz double-layer and delivers the ions for pseudocapacitance [17]. The electrolyte must be chemically inert and not chemically attack the other materials in the capacitor to ensure long time stable behavior of the capacitor's electrical parameters [17]. The electrolyte's viscosity must be low enough to wet the porous, sponge-like structure of the electrodes [17]. An ideal electrolyte does not exist, forcing a compromise between performance and other requirements [17].

There are two types of electrolytes used by EDLC manufacturers: aqueous and organic. The organic electrolyte can increase the voltage per cell compared to that of an aqueous electrolyte, therefore producing a higher energy density. The electrolyte determines the capacitor's

characteristics: its operating voltage, temperature range, ESR and capacitance [16]. With the same activated carbon electrode an aqueous electrolyte achieves capacitance values of 160 F/g, while an organic electrolyte achieves only 100 F/g [16].

Aqueous Electrolytes

Water is a relatively good solvent for inorganic chemicals [17]. Treated with acids such as sulfuric acid (H2SO4), alkalis such as potassium hydroxide (KOH), or salts such as quaternary phosphonium salts, sodium perchlorate (NaClO4), lithium perchlorate (LiClO4) or lithium hexafluoride arsenate (LiAsF6), water offers relatively high conductivity values of about 100 to 1000 mS/cm [17]. Aqueous electrolytes have a dissociation voltage of 1.15 V per electrode (2-3 V capacitor voltage) and a relatively low operating temperature range—they are used in supercapacitors with low energy density and high power density [17].

Organic Electrolytes

Electrolytes with organic solvents such as acetonitrile, propylene carbonate, tetrahydrofuran, diethyl carbonate, γ-butyrolactone and solutions with quaternary-ammonium salts or alkyl-ammonium salts such as tetraethyl-ammonium tetrafluoroborate ($(C_2H_5)_4N(BF_4)$) or triethylmethylammonium tetrafluoroborate ($C_7H_{18}BF_4N$) are more expensive than aqueous electrolytes, but they have a higher dissociation voltage of typically 1.35 V per electrode (2.7 V capacitor voltage), and a higher temperature range [17]. The lower electrical conductivity of organic solvents (10 to 60 mS/cm) leads to a lower power density, but since the energy density increases with the square of the voltage, a higher energy density [17].

Separators

Separators serve to physically separate the two electrodes; this prevents a short circuit by direct contact. It can be very thin (a few hundredths of a millimeter) and must be very porous to the conducting ions to minimize ESR [18]. Separators must also be chemically inert to protect the electrolyte's stability and conductivity [18]. Inexpensive components use open capacitor papers while more sophisticated designs use nonwoven porous polymeric films like polyacrylonitrile or Kapton, woven glass fibers or porous woven ceramic fibers [18].

2.2.2 Electric Double Layer Capacitors (EDLCs)

The Electric Double Layer

Every capacitor has two electrodes which are mechanically separated by a separator. The electrodes are electrically/ionically connected via the electrolyte: a mixture of positive and negative ions dissolved in a solvent. An area originates at the electrode surfaces where the liquid electrolyte contacts the electrode's conductive metallic surface [19, 20]. This interface forms a common boundary between two phases of matter, such as an insoluble solid electrode surface and an adjacent liquid electrolyte. In this interface occurs a special phenomenon of the double layer effect [9-22].

Double-layer capacitance is the storing of electrical energy by means of the electrical double layer effect [19, 20]. This electrical occurrence appears at the interface between a conductive electrode and a contiguous liquid electrolyte.

At the electrical double layer boundary, two layers of ions with opposing polarity form when a voltage is applied. The two layers of ions are separated by a single layer of solvent molecules that adheres to the surface of the electrode and acts like a dielectric in a

conventional capacitor—the double-layer is like the dielectric layer in a conventional capacitor, but with the thickness of a single molecule [19-22]. This makes an EDLC very stable under high field strengths (~5000 kV/mm) which may be unrealizable in conventional capacitors due to the conventional dielectric material not being able to prevent charge carrier breakthrough [19-22]. In a double-layer capacitor, breakthrough is prevented by the chemical stability of the solvent's molecular bonds. The forces that cause the adhesion of solvent molecules in the inner Helmholtz plane (IHP) are physical forces rather than chemical bonds [19, 20]. Chemical bonds exist within the adsorbed molecules, but they are polarized [19, 20]. The electrode surface area and the concentration of the adsorbed ions correlates to the magnitude of the electric charge that can accumulate in the layers.

Structure and Mechanism of an EDLC

The basic structural components of an electrochemical double layer capacitor (EDLC) consist of two carbon-based electrodes, an electrolyte and a separator. EDLCs store charge electrostatically, similar to conventional capacitors. EDLCs utilize the electrochemical double-layer that forms when voltage is applied in order to store energy. Thus, EDLCs are said to be non-Faradic, meaning that there is no transfer of charge between the electrode and the electrolyte [21].

Upon application of voltage, charge begins accumulating on the electrode surface. Ions in the electrolyte solution diffuse across the separator and fit themselves into the pores of the electrode of opposite charge. EDLC electrodes are designed to prevent the recombination of the ions, thus a double layer of charge is formed at each electrode. It is the electrode’s high surface area and the decrease in the distance between charges allowed by the double layer which enables EDLCs to achieve higher energy densities than conventional capacitors [21].

Because there is no transfer of charge between electrolyte and electrode, there are no chemical or composition changes associated with non-Faradaic processes [21]. For this reason, charge storage in EDLCs is highly reversible, which allows them to achieve very high cycling stabilities [21]. EDLCs typically possess stable performance characteristics for many charge-discharge cycles, sometimes as many as 106 cycles, while in comparison, electrochemical batteries are generally limited to only about 103 cycles [21].

Helmholtz laid the theoretical foundations of the double layer phenomenon so that it may be better expressed and understood. It is used in every electrochemical capacitor to store electrical energy [19-21]. Applying a voltage to an electrochemical capacitor causes both electrodes in the capacitor to generate electrical double layers (two layers of polarized ions). An individual double layers consist of two layers of charges: one electronic layer is in the surface lattice structure of the electrode, and the other with opposite polarity, emerges from dissolved and solvated ions in the electrolyte [19-22]. These two layers of polarized ions are separated by a monolayer of solvent molecules: the molecular monolayer forms the inner Helmholtz plane (IHP) [19-22]. The molecular monolayer adheres by physical adsorption on the electrode surface and separates the oppositely polarized ions from each other, forming a molecular dielectric [19-22]. In the process, there is no transfer of charge between electrode and electrolyte, so the forces that cause the adhesion are not chemical bonds but physical forces (e.g. electrostatic forces); thus, the adsorbed molecules are polarized but, due to the lack of transfer of charge between electrolyte and electrode, suffered no chemical changes [22]. The amount of charge in the electrode is matched by the magnitude of counter-charges in the outer Helmholtz plane (OHP) [19-22]. This is the area close to the IHP in which the polarized electrolyte ions are collected. This separation of two layers of polarized ions through the double-layer phenomena store electrical charges as in a conventional

capacitor. The double-layer charge forms a static electric field in the molecular IHP layer of the solvent molecules that corresponds to the strength of the applied voltage [19-22]. Thus, an EDLC behaves like a conventional capacitor; the amount of electric charge stored in double-layer capacitance is linearly proportional to the applied voltage and depends primarily on the electrode surface.

Materials Used in an EDLC

Electrode Material

EDLC subcategories may be distinguished principally by the form of carbon they use as an electrode material [21]. Carbon electrode materials commonly have higher surface area, lower cost, and more established fabrication techniques than other materials, such as conducting polymers and metal oxides [21]. Different forms of carbon materials that can be used to store charge in EDLC electrodes are activated carbons, carbon aerogels, and carbon nanotubes [21].

Electrolyte Material

The electrolyte used is one of the main performance parameters of an EDLC. Thus the performance can be adjusted or tuned by careful selection of the electrolyte. An EDLC can utilize either an aqueous or organic electrolyte. Aqueous electrolytes, such as H2SO4 and KOH, generally have lower ESR and lower minimum pore size requirements compared to organic electrolytes, such as acetonitrile [21]. However, aqueous electrolytes also have lower breakdown voltages [21]. Consequently, in choosing between an aqueous or organic electrolyte, one must consider the tradeoffs between capacitance, ESR, and voltage [21]. Accordingly, capacitance C is greatest in capacitors made from materials with a high permittivity ε, large electrode plate surface areas A and small distance between plates d. As a result, double-layer capacitors have much higher capacitance values than conventional capacitors, arising from the extremely large surface area of activated

carbon electrodes and the extremely thin double-layer distance on the order of a few ångströms (0.3-0.8 nm) [21, 23].

The amount of charge stored per unit voltage in an electrochemical capacitor is primarily a function of the electrode size. The electrostatic storage of energy in the double-layers is linear with respect to the stored charge, and correspond to the concentration of the adsorbed ions. Also, while charge in conventional capacitors is transferred via electrons, capacitance in double-layer capacitors is related to the limited moving speed of ions in the electrolyte and the resistive porous structure of the electrodes. Since no chemical changes take place within the electrode or electrolyte, charging and discharging electric double-layers in principle is unlimited. Real supercapacitors lifetimes are only limited by electrolyte evaporation effects.

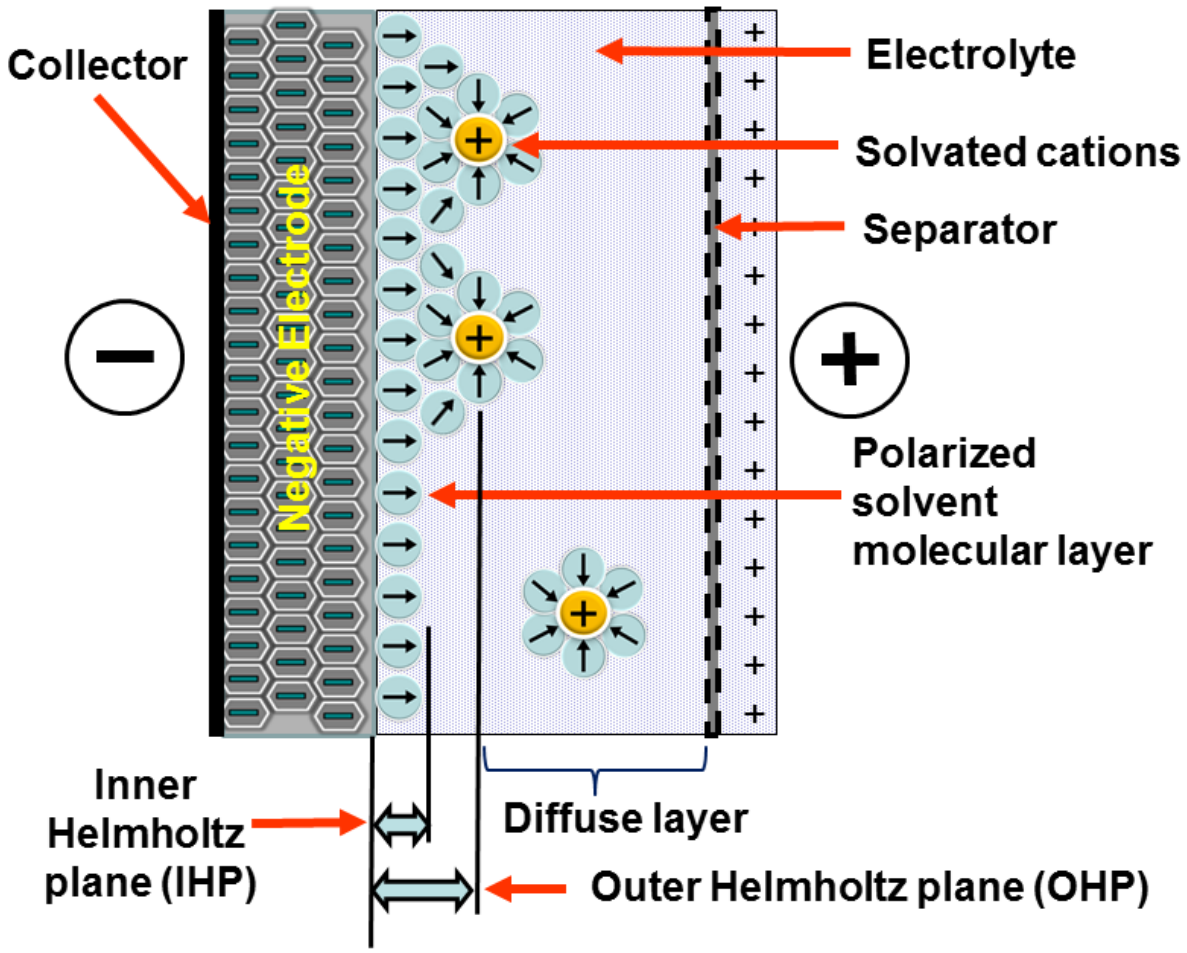

Figure 9. Electric double layer capacitor model [17].

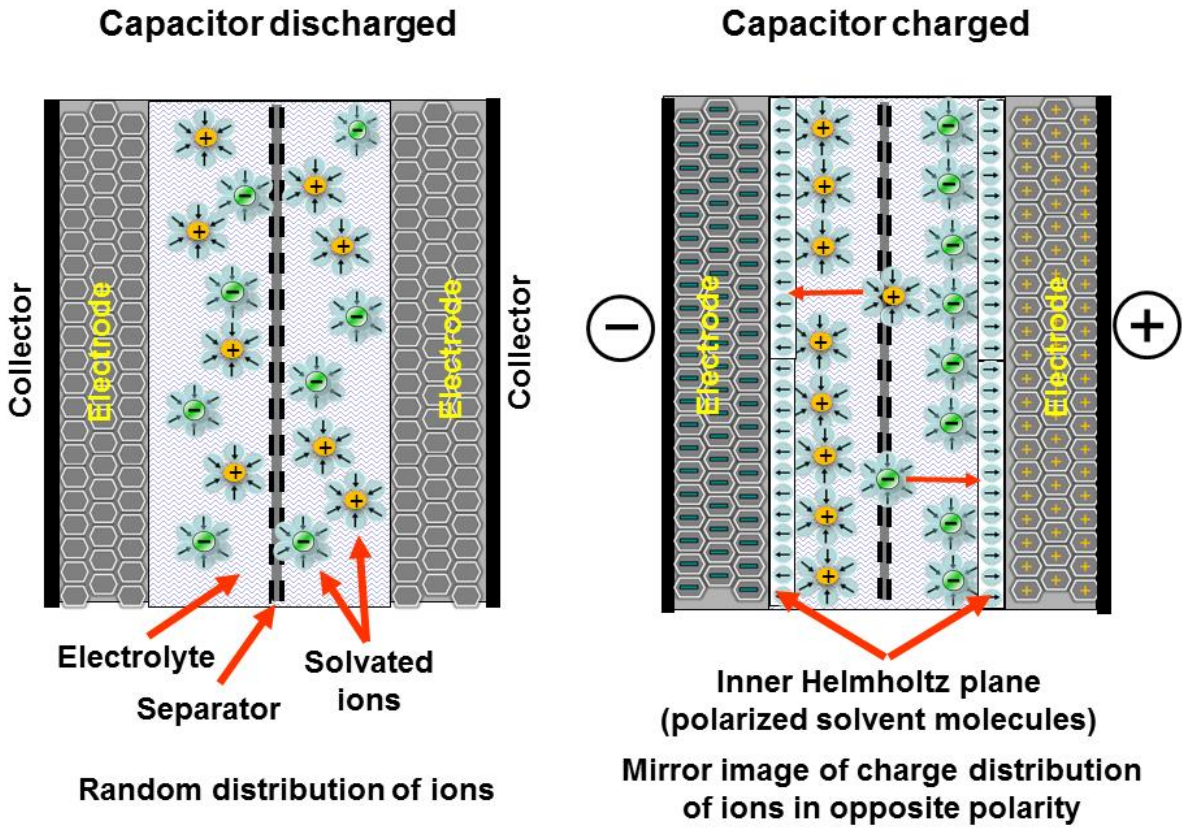

Figure 10. Electric double layer--charged and discharged states [17].

2.2.3 Pseudocapacitors

Pseudocapacitance

In contrast to EDLCs, which store charge electrostatically, pseudocapacitors store charge faradaically through the transfer of charge between electrode and electrolyte. This is accomplished through electrosorption, reduction-oxidation reactions, and intercalation processes. These Faradaic processes may allow pseudocapacitors to achieve greater capacitances and energy densities than EDLCs. There are two electrode materials that are used to store charge in pseudocapacitors, conducting polymers and metal oxides.

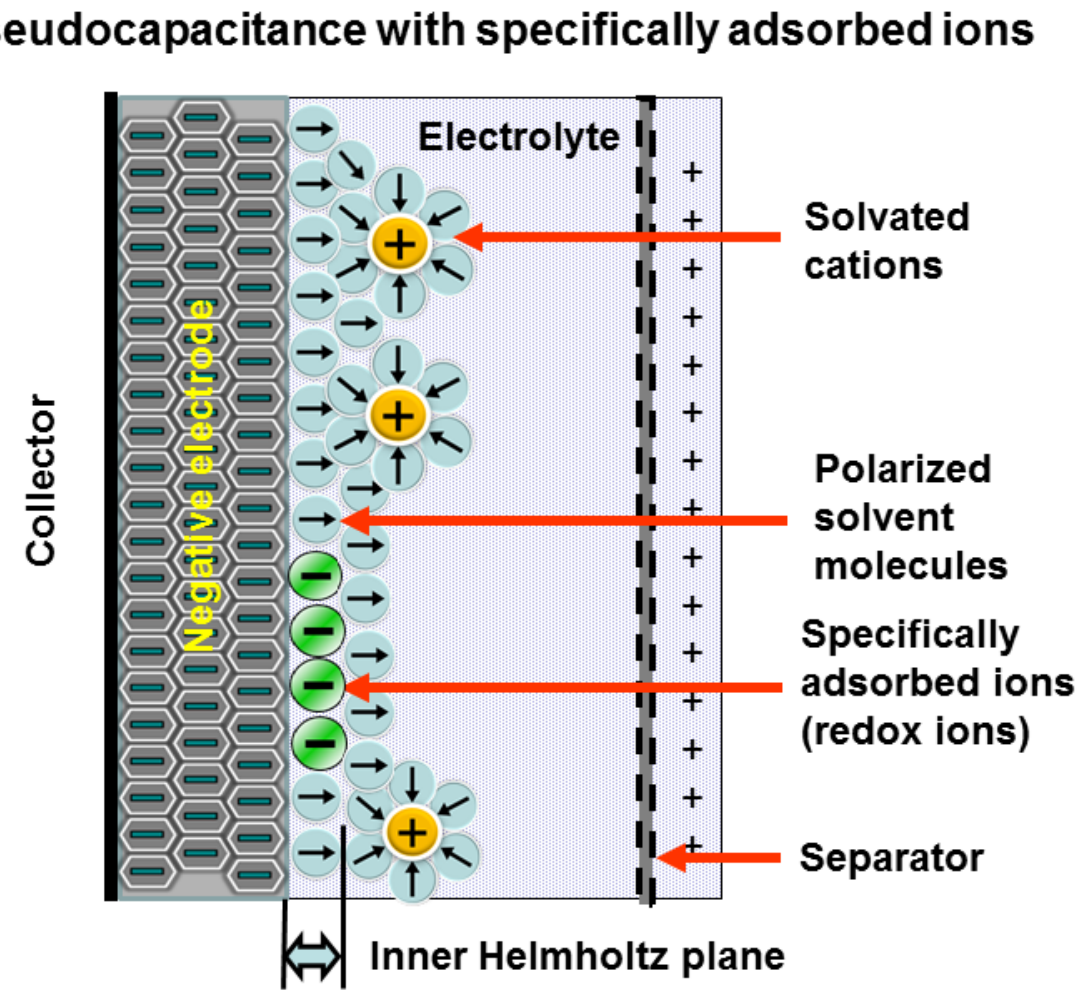

Figure 11. Pseudocapacitance model [17].

Mechanism of Pseudo-capacitance

Applying a voltage at the capacitor terminals moves the polarized ions or charged atoms in the electrolyte to the opposite polarized electrode [17, 24]. Between the surfaces of the electrodes and the adjacent electrolyte an electric double-layer forms [17, 24]. One layer of ions on the electrode surface and the second layer of adjacent polarized and solvated ions in the

electrolyte move to the opposite polarized electrode; the two ion layers are separated by a single layer of electrolyte molecules [17, 24]. Between the two layers, a static field forms that results in double-layer capacitance [17, 24]. Accompanied by the electric double-layer, some de-solvated electrolyte ions pervade the separating solvent layer and are adsorbed by the electrode's surface atoms. They are specifically adsorbed and deliver their charge to the electrode. In other words, the ions in the electrolyte within the Helmholtz double-layer also act as electron donors and transfer electrons to the electrode atoms, resulting in a faradaic current. This faradaic charge transfer, originated by a fast sequence of reversible redox reactions, electrosorptions or intercalation processes between electrolyte and the electrode surface is called pseudocapacitance [24].

Chapter 3: Literature Review

The following content in this chapter contains material from published journal articles made with the help of the author in collaboration with his colleges. The following articles are: *High-performance porous carbon/CeO2 nanoparticles hybrid super-capacitors for energy storage* [46], *Porous carbon/CeO2 composites for Li-ion battery application* [52], and *Microwave Exfoliated Graphene Oxide/TiO2 Nanowire Hybrid for High Performance Lithium Ion Battery* (accepted by the Journal of Applied Physics—not yet published).

3.1 Porous carbon/CeO2 composites for Li-ion battery application

The ever-increasing demand for portable electronic devices is the drive force behind the technological improvements in electrochemical energy storage devices such as batteries [25, 26] capacitors [27-29] and supercapacitors [30, 31]. These energy storage devices have a wide range of applications starting from wireless phones, laptops, camcorders to electric and hybrid electric vehicles. Although significant amount of research is focused on developing next generation passive sensors [32], batteries and capacitors are still the most widely used energy source for different sensors and sensor networks. Lithium-ion batteries are widely considered as the technology of choice owing to its high energy density, lightweight and flexible design and longer lifespan. Although Li is the most electropositive metal [26] (-3.04V), Li metal batteries suffered from dendritic Li growth, which led to explosion hazards, and it was necessary to find an alternative solution. Use of carbonaceous material for anode and LixMO2 for cathode material solved the issue as Li is present as Li ion rather than the metal form [26, 33], however the specific capacity and specific energy is considerably lower than the Li metal batteries. Numerous investigations have been being carried out to address this issue. Porous carbon is considered one

of the most promising materials for anode application as it has a high specific surface area (2000 m2/g), which enables higher charge-discharge rate along with high charge capacity. It has been also demonstrated that use of metal oxides nanowires or nanoparticles can increase the reversible capacity and rate capacity of a Li-ion battery (LIB) [34]. Cerium oxide (CeO2) or Ceria is a rare earth oxide that has high oxygen storage capacity, high electrical conductivity and diffusivity and high thermal stability [35, 36]. It offers high potential as an anode material for LIB due to its fast transformation between Ce(III) and Ce(IV) oxalates which have relatively low decomposition temperature in air, good structural stability and are of low cost [34]. In this work, a facile one step hydrothermal method is used to synthesize Ceria nanoparticles on Porous Carbon for LIB electrodes and the performance is compared with bare porous carbon electrodes.

3.2 High-performance Porous Carbon/CeO2 Nanoparticles Hybrid Super-capacitors for Energy Storage

The current world has an increasing demand for low cost, environment friendly and high performance energy storage/conversion systems due to the environmental problems and depletion of fossil fuels [37]. Therefore, numerous researches have been going on for the technological improvements in electrochemical energy storage devices such as batteries [38, 39] capacitors [40, 41] and super-capacitors [42]. Among available technologies, super-capacitors can be a potential electrochemical energy storage solution owing to their sustainable cycle life, higher power densities and excellent cycling stability. They are the preferred choice in wide range of applications; i.e. electric vehicles, electronic devices, airplanes and other renewable energy storage systems [43, 44]. Based on the energy storage mechanism, super-capacitors could be classified into electrical double layer capacitors (EDLC) and pseudocapacitors. In EDLC the capacitance comes from the electrostatic charge accumulation at the electrode-electrolyte interface which is a

non-faradic process; while the pseudo-capacitors store energy through fast and reversible faradic reaction which originates from the transition metal oxide or conducting polymers present in the electrode materials [37]. Numerous researches have been done on electrode materials for super-capacitors, including carbonaceous materials, transition metal oxides and conducting polymers. Each type of electrode material has its advantage and disadvantage. For instance, carbon materials work under the EDLC mechanism for charge storage and have high power density and long cycle life while transition metal oxides work under the pseudo-capacitance mechanism for charge storage and can provide higher energy density than conventional carbon materials and better cycling stability than conductive polymers [37, 45]. These unique properties of different materials have intrigued researchers to develop hybrid electrode materials via coupling carbonaceous materials and transition metal oxides as super-capacitor electrode. Coupling carbonaceous materials and transition metal oxides, gives the advantage of harnessing the best characteristics of both of these electrode materials into one hybrid electrode material. The hybrid material would thus possess the carbonaceous material's high power density and long cycle life, and the transition metal's high energy density. The hybridization of these properties is possible through the enhanced electrode/electrolyte interactions which gives the hybrid electrode material the ability to possess both SC capacitance mechanisms: EDLC (non-faradic) and pseudo-capacitance (faradic). The resulting hybrid electrode material would thus result in SCs with improved power density, energy density, cycling stability, and cycle life [37, 42, 43]. Hybrid carbon-metal oxide supercapacitors have been developed in a wide range of carbon-metal oxide combinations. Common metal oxides that have been researched include: RuO_2, MnO_2, NiO, Co_3O_4, SnO_2, ZnO, TiO_2, V_2O_5, CuO, Fe_2O_3, WO_3, etc. Not only is there a vast selection of metal oxides, there is also many forms of carbon that can be used, these include: zero-dimensional carbon (e.g. activated carbon, carbon

nanospheres, and mesoporous carbon), one-dimensional carbon nanostructures (e.g. carbon nanotubes (CNTs) and nanofibers), two-dimensional carbon nanosheets (e.g. graphene and reduced graphene oxides (rGO)), and three-dimensional carbon (e.g. porous carbon nano-architectures, 3-D porous carbon). Researchers have explored all of these areas of hybrid electrode material for use in SCs [45]. But many of the metal oxides are expensive, scarce and toxic in nature which limits their broad applications [43]. CeO_2 can be one of the most attractive candidates because of its low cost, environmental friendliness and high redox potential. As nano-particle CeO_2 could have higher pseudo-capacitive effect due to its excellent electrochemical redox characteristics [43]. A simple one step hydrothermal method for synthesizing porous carbon/CeO_2 nanoparticle (PC-CON) hybrids for super-capacitor electrode is presented here. The prepared PC-CON hybrid electrodes were investigated for super-capacitor applications within organic electrolyte and compared against pristine porous carbon electrodes. PC-CON electrode showed better performance than pristine porous carbon electrode in supercapacitor application.

3.3 Microwave Exfoliated Graphene Oxide/TiO2 Nanowire Hybrid for High Performance Lithium Ion Battery

Developing high energy density energy storage device is one of most important research goals as energy storage is the probable key solution for the utilization of alternative energy and thus for the replacement of fossil fuels and traditional energy sources [39-42, 46-48]. Lithium-ion-battery (LIB) is a potential candidate for energy storage application and LIB has wide range of applications due to its high energy density, light weight, and long cycle life [33, 39, 49, 50]. The route towards innovating future LIB depends on either synthesizing novel electrode materials or formulating a unique electrolyte with higher voltage window. Presently, graphite is widely used as anode materials for the commercial productions of LIBs but lithium storage capacity of graphite

is limited. The multilayer nature of graphite materials limits Li-ion diffusion, resulting in low charge-discharge rate performance for the battery [33, 39].

To improve the charge-discharge rate, extensive research has been done focusing on Li-ion and/or electron transport in electrode. Carbon based materials are broadly studied for LIB anode materials because of their desirable features, such as low cost, light weight, thermal and chemical stability [33, 39, 49, 51-54]. Ji et al. showed that porous carbon nanofibers have better reversible capacity and cycling performance than conventional graphite anode due to the porous structure that facilitates the ion transport [51]. Yang et al. showed that porous carbon structure is an excellent candidate for anode materials for high power density LIB [55]. In addition, various nanomaterials of metal oxides have been used as anode materials for LIB [39, 47, 52]. TiO_2 nanomaterials demonstrated its effectiveness as anode materials and this metal oxide is abundant in nature, low cost, and environmentally benign [39, 56-58]. Hybrid nanostructures electrodes which interconnect nanostructured electrode materials with conductive additive nanophases, is another way of improving Li-ion insertion properties [39, 50, 59]. For example, hybrid nanostructures, such as Mn3O4-graphene hybrids or LiFePO4-RuO2 nano-composite, combined with conventional carbon additives (e.g., acetylene black), have demonstrated an increased Li-ion insertion/extraction capacity in hybrid electrodes at high charge/discharge rates [47, 60].

Graphene, a single layer of graphite with perfect 2D crystal of sp2 hybridized carbon atoms, has been found to have extraordinary properties that could further enhance LIB performance. It has high specific surface area (2600 m2/g) and can sustain at a current density up to six times that of copper [33, 39, 47, 61, 62]. Therefore, graphene has been found as the ideal conductive additive for hybrid nanostructured electrode. However, synthesizing graphene through

chemical vapor deposition (CVD) method or thermal reduction of graphene oxide is expensive and time consuming, leading to high cost and limited scale application.

A highly efficient and low cost synthesize method of fabricating a hybrid anode structure using microwave exfoliated graphene oxide (MEGO) and TiO_2 nanowires is presented here. The MEGO was obtained through microwave treatment of solution processed graphene oxide (GO). Later, a simple hydrothermal method was utilized to obtain TiO_2 nanowires on exfoliated graphene oxide sheet. This obtained microwave exfoliated graphene oxide/TiO_2 nanowire (MEGO-TON) hybrid electrode material was compared with porous carbon (PC). The MEGO-TON hybrid has shown higher reversible capacity and rate capacity than PC when used in LIB as anode material. This simple hybrid anode material synthesis method has the potential to be utilized for large-scale anode material production for LIBs.

Chapter 4: Experimental Methods

The following content in this chapter contains material from published journal articles made with the help of the author in collaboration with his colleges. The following articles are: *High-performance porous carbon/CeO2 nanoparticles hybrid super-capacitors for energy storage* [46], *Porous carbon/CeO2 composites for Li-ion battery application* [52], and *Microwave Exfoliated Graphene Oxide/TiO2 Nanowire Hybrid for High Performance Lithium Ion Battery* (accepted by the Journal of Applied Physics—not yet published).

4.1 Porous carbon/CeO2 composites for Li-ion battery application

Porous Carbon/Cerium oxide nanoparticle (PC/CON) hybrids Synthesis

The PC/CON hybrid synthesis is a one-step hydrothermal method. At first 100 mg Porous Carbon (ACS Material, LLC) was dispersed in 200 mL of deionized (DI) water. Then 150mL of 0.02M Ammonium Cerium Nitrate $(NH_4)_2Ce(NO_3)_6$ was added to the solution and the solution was sonicated for 45 minutes. The mixture was then separated by centrifugation. At this stage $Ce(OH)_4$ was formed on the pores and surfaces of the porous carbon. Then the product was mixed with 100 mL 5M NaOH solution and transferred into a Teflon lined autoclave. After heating the mixture for 45 hours at 180° C, the solution was separated by centrifugation, washed with DI water for three times. Then the remnant was dried at 70° C. At last the product was heated at 450° C in Argon for 2 hours [44, 63]. A schematic of the synthesis procedure is depicted in Figure 12.

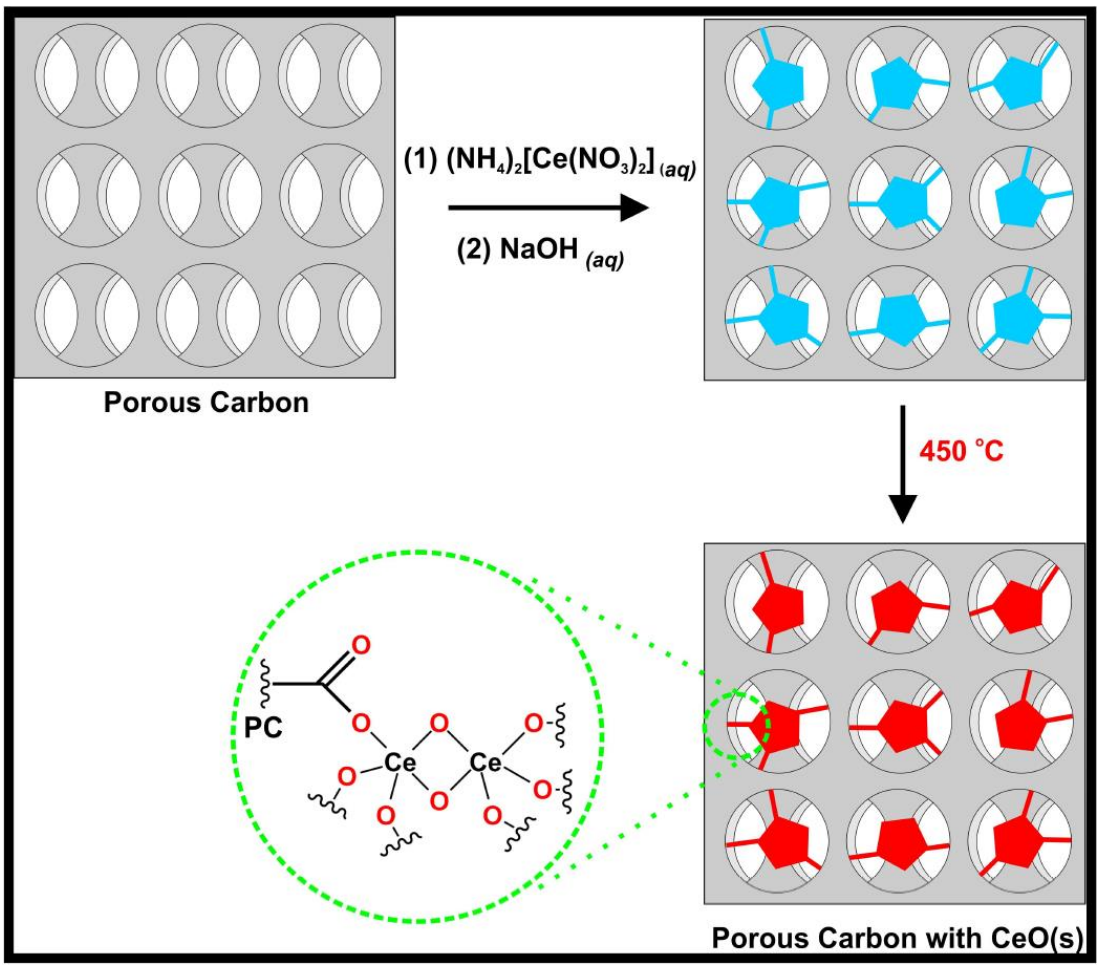

Figure 12. Schematic of CeO2 synthesis on porous carbon.

Anode Preparation

For making anodes for both PC and PC-CON electrodes, Polyvinylidene Fluoride (PVDF, MTI corp., purity ≥99.5%) was used as binding material. PVDF was dissolved in N-Methyl-2-pyrrolidone (NMP, MTI corp., purity ≥99.5%) at a 1:2.5 weight ratio by heating at 80 °C. Later 80 wt% active material and10 wt% activated carbon were dispersed in 10 wt% PVDF with excess NPM to prepare homogenous slurry using a homogenizer. Then the slurry was coated on Copper foil and dried at 100 °C on a hot plate. Next, a precision disc cutter from MTI Corporation was used to cut anodes with 13 mm diameter. Later the anodes were kept overnight in vacuum oven.

Coin Cell Assembly

Coin cells (CR 2032) were assembled using either PC anodes or PC-CON anodes inside an Argon filled glovebox (Unilab, MBraun). Oxygen and moisture level were kept less than 0.1 ppm inside the glovebox. One molar $LiPF_6$ in ethylene carbonate (EC), dimethyl carbonate (DMC), and diethyl carbonate (DEC) organic solvent at 1:1:1 volume ratio was used as electrolyte as received (MTI corp.). Celgard 2500 was used as the separator. A cross-sectional view for coin cell assembly is shown in Fig. 13.

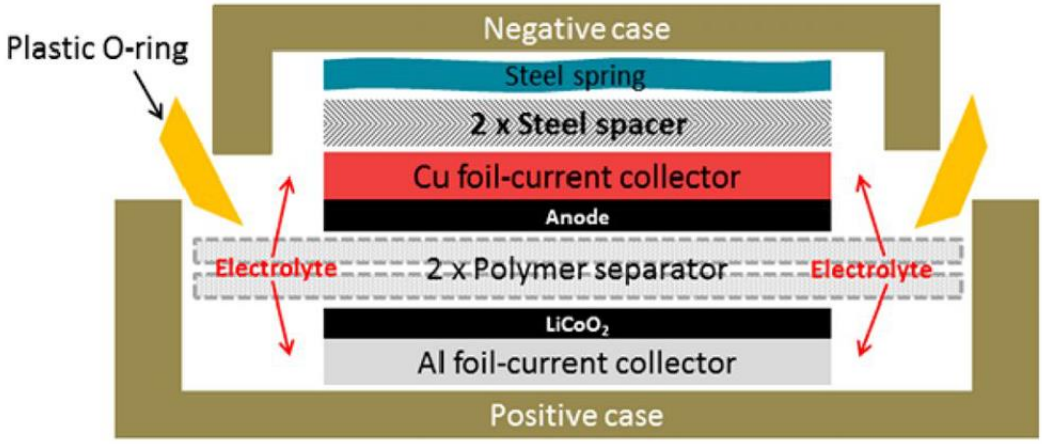

Figure 13. Cross-sectional view of coin cell assembly.

4.2 High-performance Porous Carbon/CeO2 Nanoparticles Hybrid Super-capacitors for Energy Storage

Porous carbon/cerium oxide nanoparticle (PC-CON) hybrids synthesis

The porous carbon/cerium oxide nanoparticle (PC-CON) hybrid synthesis method used to make the supercapacitor's active material is the same method used to make the active material for the lithium-ion battery application. The steps for this synthesis method can be seen on Fig. 12.

Electrode fabrication

A two electrode testing set up was prepared using coin cells (CR 2032) because it provides most accurate measure for an electrode's performance for electrochemical capacitors [71]. For making both PC and PC-CON electrodes, polyvinylidene fluoride (PVDF, MTI corp., purity ≥99.5%) was used as binding material. PVDF was dissolved in N-Methyl-2-pyrrolidone (NMP, MTI corp., purity ≥99.5%) at a 1:2.5 weight ratio by heating at 80 °C. Later 80 wt% active material and10 wt% activated carbon were dispersed in 10 wt% PVDF with excess NPM to prepare homogenous slurry using a homogenizer. Then the slurry was coated on Aluminum foil and dried at 100 °C on a hot plate. Then a precision disc cutter from MTI Corporation was used to cut anodes with 13 mm diameter. Next the pieces were kept overnight in vacuum oven.

Coin cell assembly

Coin cells (CR 2032) were assembled using either PC electrodes or PC-CON electrodes inside an Argon filled glovebox (Unilab, MBraun). One molar Tetraethylammonium tetrafluoroborate ($TEABF_4$) (Sigma Aldrich) in acetonitrile was prepared inside the glovebox for the electrolyte. Polypropylene membrane (Celgard) was used as separator. Oxygen and moisture level were kept less than 0.1 ppm inside the glovebox.

4.3 Microwave Exfoliated Graphene Oxide/TiO_2 Nanowire Hybrid for High Performance Lithium Ion Battery

Synthesis of graphene oxide

Improved Hummer's method was utilized for the synthesis of GO [12]. A 9:1 mixture of concentrated H_2SO_4/H_3PO_4 (360:40 ml) (Fisher Scientific/EM Science, respectively) was added

to a mixture of graphite flakes (3.0 g, 1wt. equiv.) (Alfa Aesar, natural, 10 mesh, 99.9%) and $KMnO_4$ (18.0 g, 6 wt. equiv.) (Fisher Scientific). The reaction was then heated to 50˚C in a water bath and stirred for 12 hrs. The reaction was cooled to room temperature and poured onto ice and D.I. water mixture (~400 ml) with 30% H_2O_2 (3 ml). The mixture was then thoroughly mixed and centrifuged to decant away supernatant. The remaining solid material was then washed in succession with 200 ml of water, 200 ml of 30% HCl (diluted: 37.3% Assay, Fischer Scientific), and then several general washes with water. The remaining solid material was vacuum dried overnight at 50˚C.

Microwave exfoliation of graphene oxide (MEGO)

GO obtained from improved Hummer's method were treated in a microwave oven (Haier, Model: MWMM0701TB) in ambient condition at 700 W for 1 min. A large volume expansion of GO was observed. Due to the microwave radiation the GO was exfoliated and became fluffy black powder which indicates reduction of the GO.

Synthesis of TiO2 nanowires on MEGO

The TiO_2 nanowires were synthesized following a simple hydrothermal method [68]. Microwave reduced graphene oxide (0.5 g) was transferred to a 250 mL Pyrex glass bottle and mixed with a 100 mL solution containing DI water and concentrated hydrochloric acid (HCl, 37.3% Assay, Fischer Scientific) in a 1:1 volume ratio. Subsequently, 5 mL of the titanium tetrachloride (99.0% purity, Sigma Aldrich) was added drop-wise to this solution. The glass bottle was then placed inside and aluminum cylinder and transferred into an oven at 160 °C for 4 hours. After that, the resulting materials were rinsed several times with DI water and dried at 90 °C for 30 minutes.

The as-prepared samples were characterized using powder X-ray diffraction (XRD, B8 Discover, Bruker) and scanning electron microscopy (SEM, S-4800, Hitachi). In the above reaction condition, the formation of TiO_2 nanowires takes place as follows-

$$TiCl_4 + H_2O \rightarrow \text{Ti (IV) complex}$$

$$2\text{Ti (IV) complex} \xrightarrow{\text{dehydration}} TiO_2$$

Later the obtained materials were heated at 450 °C for 2 hours in Argon environment for complete reduction of the MEGO.

Anode preparation

For making anodes for both PC and MEGO-TON hybrid electrodes, Polyvinylidene Fluoride (PVDF, MTI corp., purity ≥99.5%) was used as binding material. PVDF was dissolved in N-Methyl-2-pyrrolidone (NMP, MTI corp., purity ≥99.5%) at a 1:2.5 weight ratio by heating at 80 °C. Later 80 wt% active material and 10 wt% activated carbon were dispersed in 10 wt% PVDF with excess NPM to prepare homogenous slurry using a homogenizer. Then the slurry was coated on Copper foil and dried at 100 °C on a hot plate. Next, a precision disc cutter from MTI Corporation was used to cut anodes with 13 mm diameter. Later the anodes were kept overnight in a vacuum oven. The anode preparation view is schematically shown in Figure 14.

Coin Cell Assembly

Coin cells (CR 2032) were assembled using either PC or MEGO-TON hybrid as electrodes and lithium metal foil as counter electrode inside an Argon filled glovebox (Unilab, MBraun). Oxygen and moisture level were kept less than 0.1 ppm inside the glovebox. One molar $LiPF_6$ in ethylene carbonate (EC), dimethyl carbonate (DMC), and diethyl carbonate (DEC) organic solvent

at 1:1:1 volume ratio was used as electrolyte as received (MTI corp.). Celgard 2500 was used as the separator. A schematic view for coin cell assembly is shown in Fig. 14.

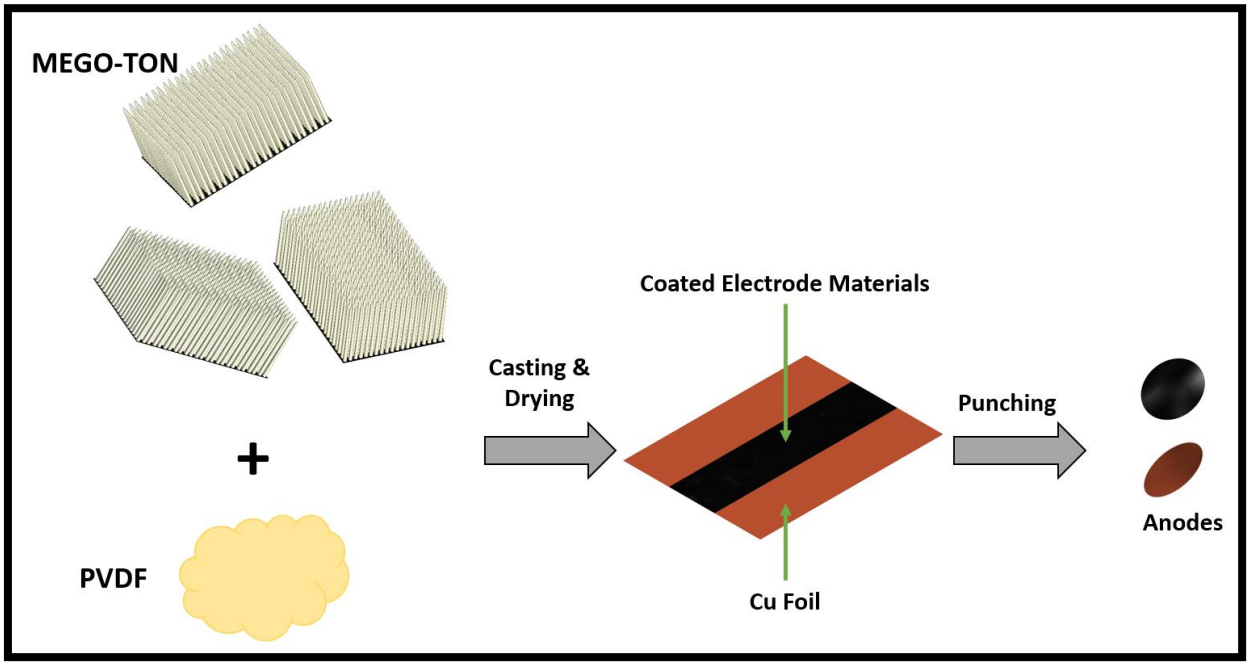

Figure 14. Schematic view of anode preparation.

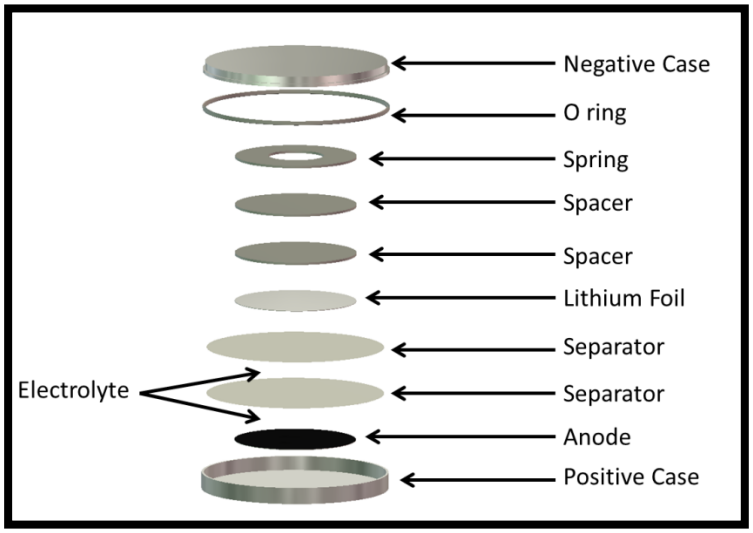

Figure 15. Schematic view of coin cell assembly.

Chapter 5: Results and Discussion

The following content in this chapter contains material from published journal articles made with the help of the author in collaboration with his colleges. The following articles are: *High-performance porous carbon/CeO2 nanoparticles hybrid super-capacitors for energy storage* [46], *Porous carbon/CeO2 composites for Li-ion battery application* [52], and *Microwave Exfoliated Graphene Oxide/TiO2 Nanowire Hybrid for High Performance Lithium Ion Battery* (accepted by the Journal of Applied Physics—not yet published).

5.1 Porous carbon/CeO2 composites for Li-ion battery application

Material Characterization

Scanning Electron Microscopy (SEM) and Transmission Electron Microscopy (TEM) were used to determine the size and the morphology of the PC-CON hybrids as shown in Figure 16. As indicated by the figure, CeO_2 particles were formed on the surfaces and nooks of the porous carbon. The nanoparticles had a diameter between 6 to 8 nm. Clear lattice fringes were observed in HRTEM image which confirms the formation of crystalline particles formed in the hydrothermal reaction.

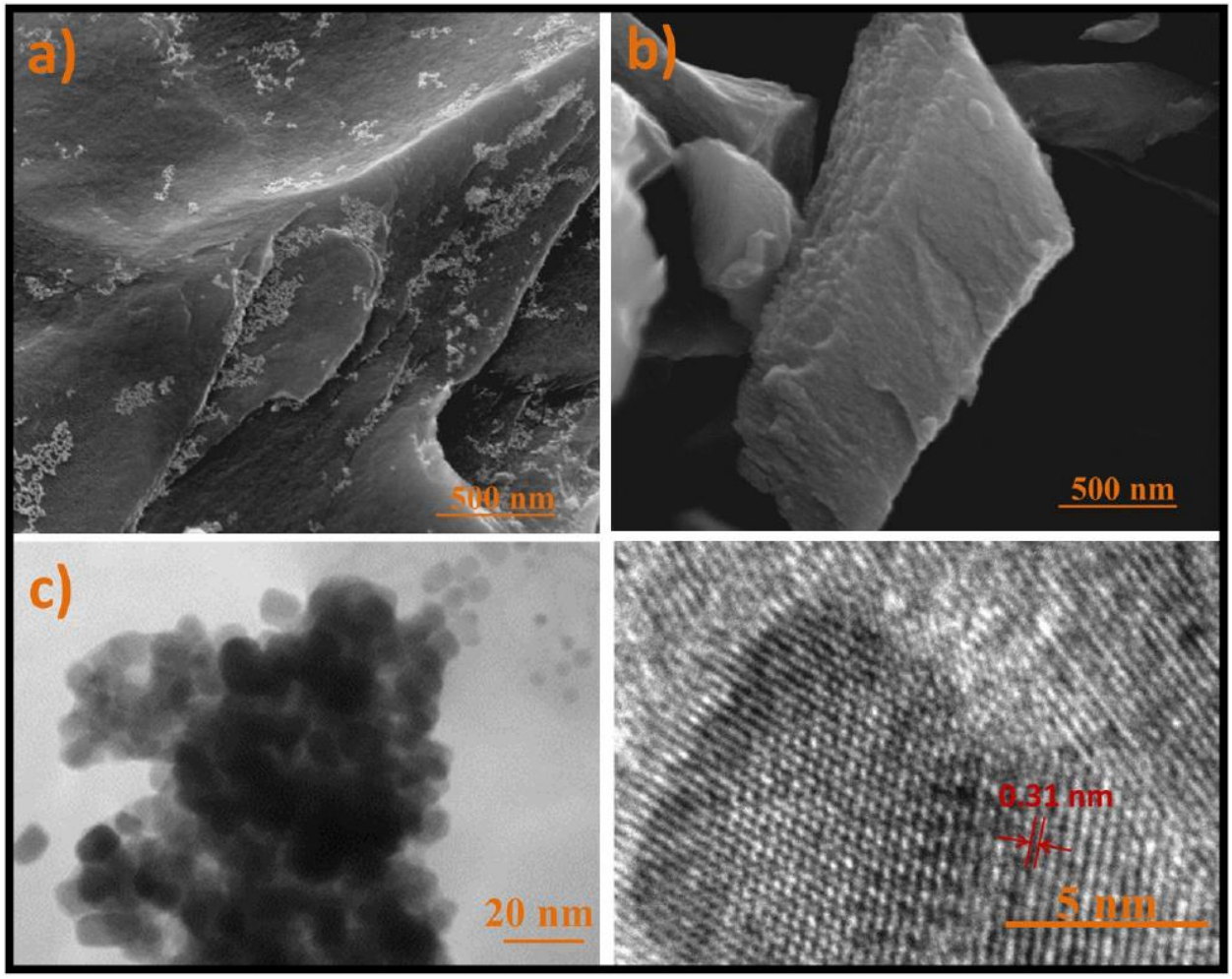

Figure 16. (a) SEM image of CeO_2 nanoparticles on porous carbon, (b) morphology of porous carbon, (c-d) TEM and HRTEM images of CeO_2 nanoparticles.

The crystal structures of the PC/CON hybrid were determined utilizing a Bruker D8 Discover XRD using Cu Kα radiation. The asterisk (*) marked peak represents porous carbon and rest of the XRD peaks indicate that the products were well crystallized and have a cubic fluorite structure of CeO2 (space group: Fm3m) with lattice constant a=5.411Å, which is in agreement with the JCPDS file for CeO2 (JCPDS 34-0394). No extra peaks corresponding to any other secondary phases were observed.

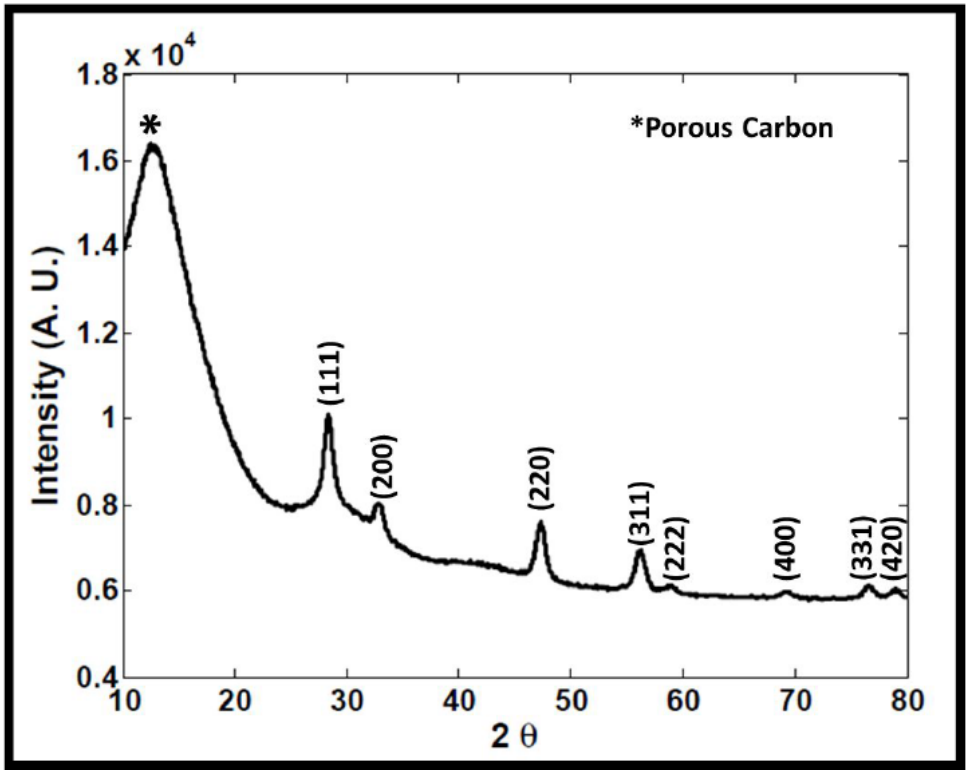

Figure 17. XRD result PC-CON. Asterisk (*) peak is for porous carbon. The rest of the peaks belong to CeO_2.

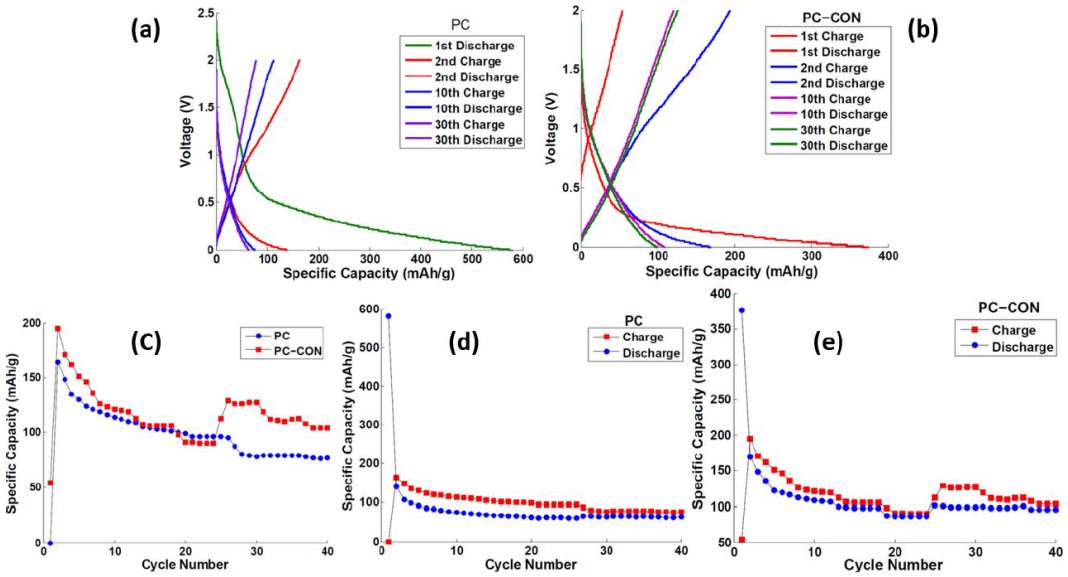

Figure 18. Measurements of capacity and rate capability, (a) charge/discharge curve for PC anode, (b) charge/discharge curve for PC-CON anode, (c) comparison of specific capacity of the two anode materials as a function of cycle number: PC anode was cycled at 100 for 40 cycles; PC-CON was varied among 100mA/g, 200mA/g, 300mA/g and 500mA/g consecutively after every 5 cycles (d) cycling performance of PC anode at 100mA/g for 40 cycles (e) specific capacity of PC CON at 100mA/g, 200mA/g, 300mA/g and 500mA/g consecutively after every 5 cycles.

Anode Testing

To evaluate the electrochemical performance of the anodes an eight-channel battery analyzer form MTI Corporation was used. Figure 18 (a) and (b) shows the galvanostatic charge-discharge curves for PC and PC/CON anodes respectively at the voltage window between 0.01 to 2 V in the 1st, 2nd, 10th and 30th cycles. The significantly high value of capacity in the first discharge is caused largely by the decomposition of the non-aqueous electrolyte and the formation of solid electrolyte interface (SEI) layer on the electroactive materials [34]. This is also would likely to protect the electrodes partly and improve the stability of cyclic performance [34, 65]. The current density used for the PC electrodes is 100 mA/g while for PC/CON electrode it was varied from 100mA/g, 200 mA/g, 300 mA/g and 500mA/g in a cyclic manner. It can be seen that while the electrode with only PC shows a capacity of 64 mAh/g at the 30th cycle, the PC/CON electrode

retained capacity around 100 mAh/g after that cycle. Fig. 18 (c) compares the specific capacity of the PC and PC/CON electrodes as a function of cycle number from 2nd cycle to the 40th cycle at different current densities. The capacity of PC electrode decreased from 164 mAh/g to 77 mAh/g while PC/CON showed a higher capacity of 195 mAh/g in the 2^{nd} cycle and it went down to 146 mAh/g and then successively to 90 mAh/g with further increase in current densities. However, when the current density was returned to the 100 mA/g the electrode recovered to 113 mAh/g capacity. After the 40th cycle, PC/CON electrode showed significantly higher capacity (104 mAh/g) over the PC electrode (77 mAh/g) although it was measured at five times higher current density (500 mA/g).

5.2 High-performance Porous Carbon/CeO2 Nanoparticles Hybrid Super-capacitors for Energy Storage

Material Characterization

The active material characterized for the porous carbon/cerium oxide hybrid is the same material used for the lithium-ion battery application. Thus, the same characterization methods and results were exhibited. Characterization results can be seen in Figure 16 and 17.

Electrode Testing

To understand the electrochemical behavior for the PC and PC-CON electrode materials, cyclic voltammetry (CV) and galvanostatic charge/discharge were carried out in 1M $TEABF_4$ in acetonitrile electrolyte solution assembling two electrode testing set up as coin cells. A potentio-galvanostat from EZ-stat was used for all the testing. Figure 19 (a-b) shows cyclic voltammetry for the two samples at different scan rates of 100mV/s, 250mV/s, 400mV/s and 500mV/s with a scan range between 0 to 2.2V. The area under each CV curve suggests that all fabricated supercapacitor have good electrochemical stability and capacitance [31]. Figure 19 (e) shows the

comparison of CV plot at 100mV/s scan rate for both samples and the area under the CV curve for PC-CON sample is larger than the PC sample which suggests that the PC-CON sample has higher specific capacitance [66]. Moderate leakage resistance of each sample was perceived as low leakage resistance would skew all CV curves vertically [31]. Pseudo-capacitive behavior of all samples had been observed which can be ensured by the mirror like image at the anodic and cathodic regimes [66].

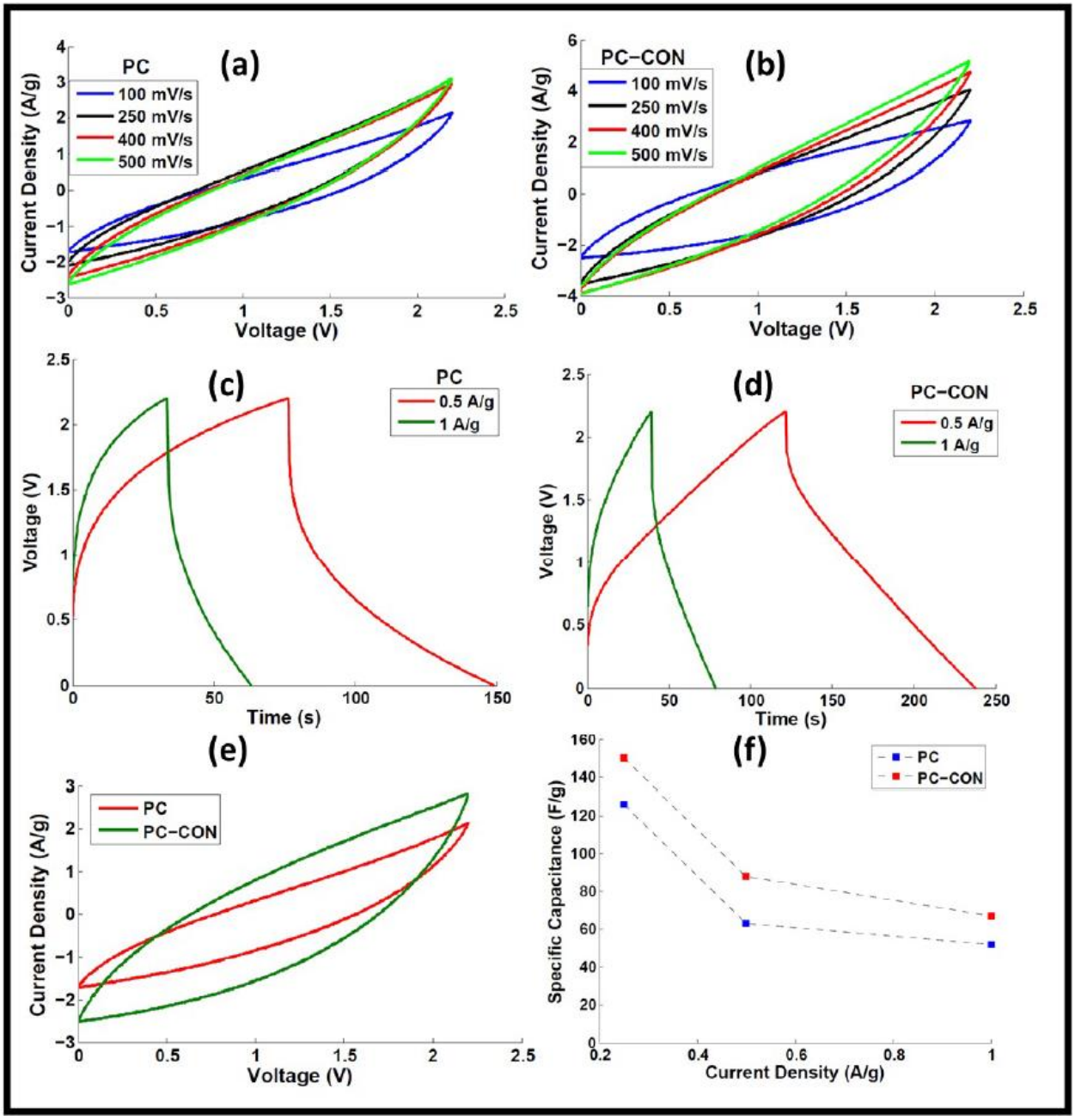

Figure 19. (a) & (b) Cyclic voltammetry of PC and PC-CON at different scan rates in 1M TEABF4 and in acetonitrile, (c) & (d) galvanostatic charge discharge profiles of PC and PC-CON, (e) comparison of CV plot for PC and PC-CON at 100mV/s scan rate, (f) specific capacitance of PC and PC-CON at different current density.

Figure 19 (c-d) shows the galvanostatic charge discharge curves for PC and PC-CON at 0.5A/g and 1A/g within the potential window of 0-2.2V. The charging-discharging curve for PC-

CON sample showed more symmetric nature than PC sample indicating better electrochemical capacitive property and high reversibility, consistent with earlier CV observation. Specific capacitance for the super-capacitors was calculated by the following equation [31, 67]:

$$C_s = \frac{4I}{m}\frac{\Delta t}{\Delta V}$$

where *I* is the discharging current, *t* is the discharging time, *V* is the discharging voltage, and *m* is the total mass of active material in both electrodes. Figure 19 (f) shows the specific capacitance for both samples at 0.25A/g, 0.5A/g and 1A/g current density. The calculated specific capacitance for PC sample was 126F/g and for PC-CON sample was 150F/g at current density of 0.25A/g. For the current density 0.5A/g and 1A/g, the specific capacitance of PCCON sample was also higher than PC sample. As the current density increased, the specific capacitance decreased for all the samples. A slopped variation in potential vs. time (1.8-2.2V) indicates typical pseudo-capacitance behavior caused by the electrochemical absorption/desorption or a redox reaction at the electrode-electrolyte interface [43]. Clearly, the specific capacitance of the PC-CON sample is significantly larger than the specific capacitance of PC sample which is in good agreement with CV curves. Indeed, the introduction of CeO_2 nanoparticle in porous carbon produces a positive synergistic effect to significantly increase its utilization for high capacitance.

5.3 Microwave Exfoliated Graphene Oxide/TiO_2 Nanowire Hybrid for High Performance Lithium Ion Battery

The surface morphology of the MEGO is shown in Figure 20 (a) and the surface topography is curvy and rough, indicating high surface area of the MEGO. As indicated by Figure

20 (c) and (d), TiO_2 nanowires are uniformly grown on MEGO with an average diameter of 200 nm and length of 3 μm. Because of the wavy nature of MEGO, TiO_2 nanowires growth followed its surface topography, indicating the MEGO morphology was maintained after the nanowire growth. Figure 20 (b) shows the morphology of the pristine PC (CAS No 7440-44-0) purchased from ACS Material.

XRD analysis on the MEGO-TON hybrid utilizing a XRD (B8 Discover, Bruker) is shown in Figure 21. All the peaks matched with the standard diffraction data of rutile TiO_2 (JCPDS, No. 76-1940). XRD patterns exhibited strong diffraction peaks at 27°, 36° and 55° indicating TiO_2 in the rutile phase. No extra peaks corresponding to any other secondary phases were observed [68].

Fourier transform infrared (FTIR) spectra were obtained by using a Perkin-Elmer, Spectrum 100, Universal ATR Sampling Accessory with the range of 650−3650 cm^{-1} in transmittance mode. Figure 22 shows the neat FTIR spectra of GO and MEGO. The FTIR of GO shows the presence of C=O stretching at 1728 cm^{-1}, graphene sheet aromatic C=C stretching at 1622 cm^{-1}, broad O–H stretching at 3400 cm^{-1}, C-OH bending at 1368 cm^{-1}, C-O stretching at 1045 cm^{-1}, and C–OH stretching at 1222 cm^{-1}. The FTIR spectrum of GO revealed the presence of oxygen containing functional groups in it such as –COOH, –OH, epoxide and alcoxide. On the other hand, the FTIR spectrum of MEGO shows the presence of C=O stretching at 1734 cm^{-1}, graphene sheet aromatic C=C stretching at 1628 cm^{-1} which may have overlapped with other absorptions leading to a slightly broader absorption centered at 1576 cm^{-1}. Moreover, the presence of absorption band ranging from 950 to 1350 cm^{-1} is due to the presence of epoxy and alcoxy groups in the MEGO. Usually, the epoxy and alcoxy stretching absorption (C–O) are seen at 1288 and 1076 cm^{-1} respectively. All of these absorption bands of PRGO IR spectra indicate the presence of very low amount of oxygen containing functional groups in it compared to the GO

sample. The absence of O-H stretching 3400 cm^{-1}, C-OH bending at 1368 cm^{-1}, C-O stretching at 1045cm^{-1} and C–OH stretching at 1222 cm^{-1} all indicates that the MEGO contains no or very low –COOH and –OH functional groups [69].

To evaluate the electrochemical performance of the electrodes, we investigated the Li-ion insertion/extraction properties in PC and MEGO-TiO_2 hybrid materials using MTI eight-channel battery analyzer. Figure 23 (a) shows the galvanostatic charge-discharge curves for PC electrode within the voltage window 0.01 to 2 V in the 1st, 2nd, 25th, and 40th cycles; Figure 23 (b) shows the similar curves for MEGO-TiO_2 hybrid electrode within the same voltage window in the 1st, 2nd, 25th, and 40th cycles. The current density for both electrodes was maintained at 100mA/g, 200mA/g, 300mA/g, and 500 mA/g respectively for 40 cycles. The current density was shifted for every 5 cycles. Note that no obvious voltage plateau was observed for both cases. The significantly high value of capacity in the first discharge is caused largely by the decomposition of the non-aqueous electrolyte and the formation of solid electrolyte interface (SEI) layer on the electroactive materials. This would also likely to protect the electrodes partly and improve the stability of cyclic performance [70, 71]. Figure 23 (c) shows the cyclic performance for PC and MEGO-TON hybrid electrode. As mentioned before, the cycling stability of PC and MEGO-TON hybrid electrodes were measured at varied current density within the range of 100-500 mA/g for 40 cycles. For both sample, the specific capacity decreased with the increase of current density. With the increase in cycle numbers lithium storage performance of PC electrode drops. After 11th cycle, specific capacity for PC anode was 78 mAh/g then reduced to 72 mAh/g after 35th cycle at the same current density (300 mA/g). On the contrary, the specific capacity of MEGO-TON anode was 109 mAh/g then became 111 mAh/g after 35th cycle at similar current density. For the first 20 cycles at current density 100, 200, 300, and 500 mAh/g the specific capacity of MEGO-TON

sample was respectively 38%, 38%, 39%, and 56% higher than PC anode. For the next 20 cycles, the specific capacity for MEGO-TON sample was respectively 17%, 40%, 55%, and 80% higher than PC sample at similar order of current density. Note that, with the percentage increment of specific capacity for MEGO-TON sample becomes more at higher current density. This increment is due to the TiO_2 nanowires, because all other testing parameters for both batteries are same and same testing parameter is used. It can be explained that charge-discharge cycles create more space to facilitate Li-ion diffusion, augmenting the specific capacity for MEGO-TON anode as the cycle number increases. Lower capacity in the beginning resulted from the incomplete reaction and irreversible lithium loss due to the formation of solid electrolyte interface.

Previously, it was shown that graphene electrode has lower performance than graphene/metal oxide nanowire hybrid electrode because metal oxide nanowires prevent the graphene sheets from agglomerating, preserving high surface area which is favorable for Li-ion storage [33]. Though the PC's porous structure helps for high rate performance by facilitating ion transport, it can be anticipated from the electrochemical results of MEGO-TON hybrid sample that the TiO_2 nanowires provide better elastic buffer space for Li-ion during intercalation/deintercalation, which prevents cracking or crumbling of the electrodes retaining the original properties. Moreover, graphene has high electrical conductivity which benefits the MEGO-TON hybrid electrode in achieving low resistance and electronic/ionic conductivity, therefore leading to a higher specific capacity. Finally, MEGO-TON hybrid electrode provides large electrode/electrolyte contact area and short path length for Li-ion diffusion with good stability, thus further facilitates the Li-ion transport. All above-mentioned reasons are expected to be responsible for the improved anodes with excellent energy storage capacity, cycling stability, and Coulombic efficiency.

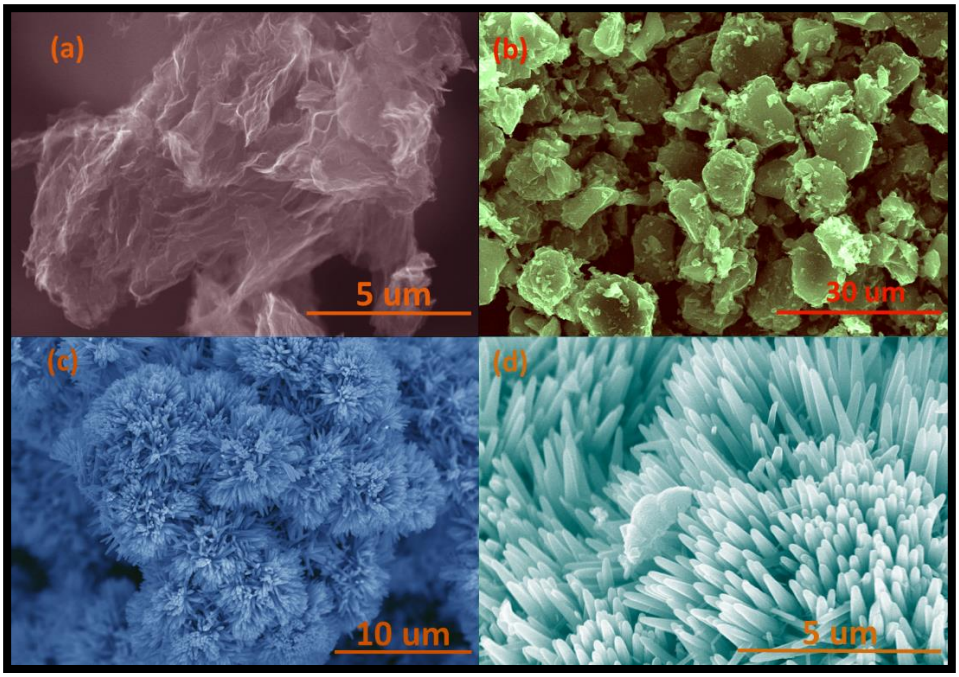

Figure 20. SEM image of (a) MEGO, (b) PC, (c-d) MEGO-TON hybrid.

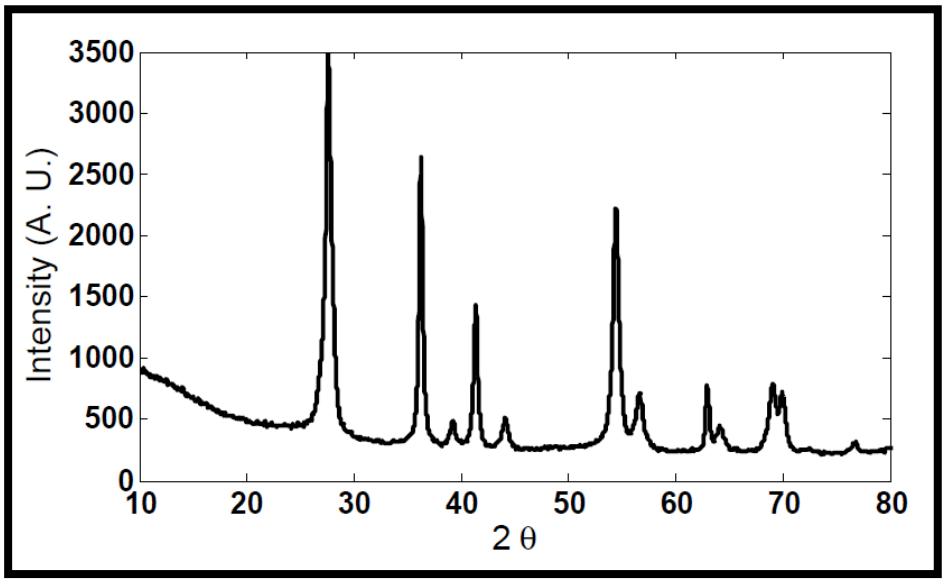

Figure 21. XRD result for MEGO-TON hybrid.

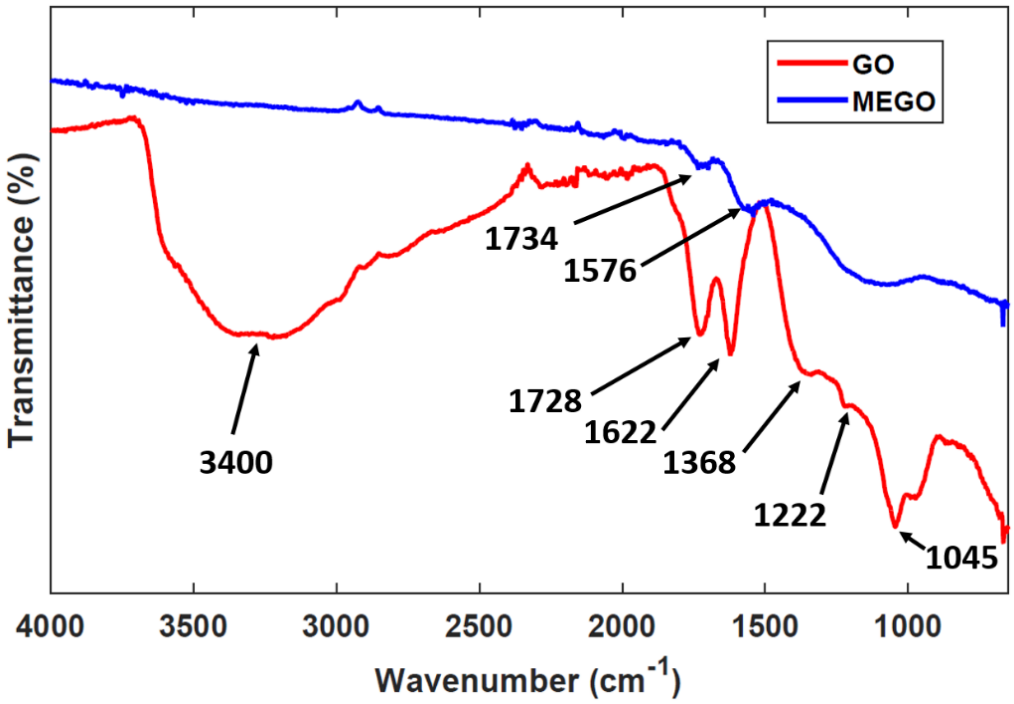

Figure 22. FTIR spectra of GO and MEGO.

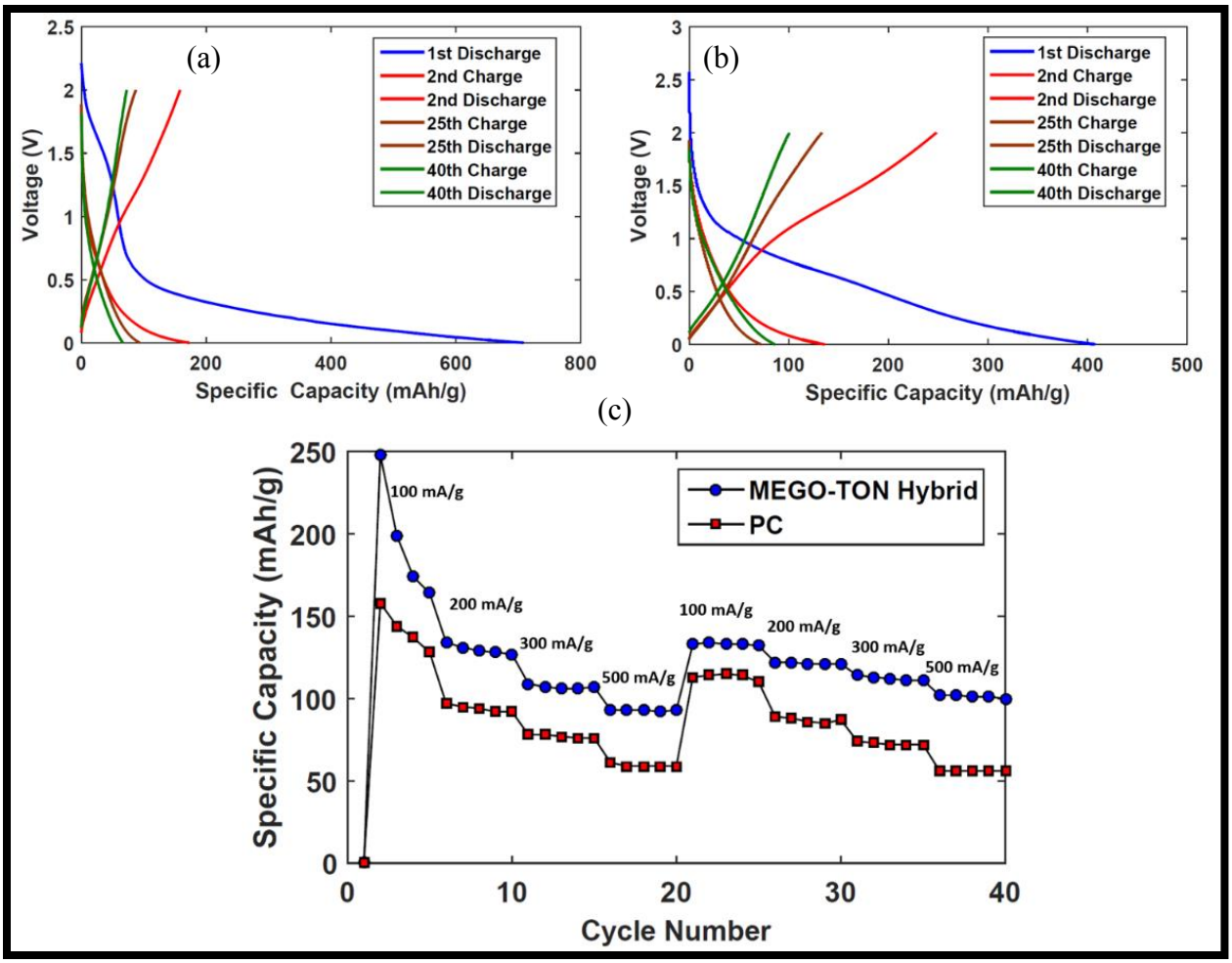

Figure 23. Measurements of capacity and rate capability, (a) charge/discharge curve for PC electrode, (b) charge/discharge curve for MEGO-TON hybrid electrode, (c) comparison of specific capacity of the two anode materials as a function of cycle number: P PC and MEGO-TON anode were cycled at 100mA/g, 200mA/g, 300mA/g, and 500 mA/g current density respectively for 40 cycles.

Chapter 6: Conclusion

The following content in this chapter contains material from published journal articles made with the help of the author in collaboration with his colleges. The following articles are: *High-performance porous carbon/CeO2 nanoparticles hybrid super-capacitors for energy storage* [46], *Porous carbon/CeO2 composites for Li-ion battery application* [52], and *Microwave Exfoliated Graphene Oxide/TiO2 Nanowire Hybrid for High Performance Lithium Ion Battery* (accepted by the Journal of Applied Physics—not yet published).

6.1 Porous carbon/CeO2 composites for Li-ion battery application

In summary, a single step hydrothermal synthesis technique was utilized to synthesize Ceria nanoparticles on porous carbon to develop a high performance LIB anode material. The growth and presence of Ceria was confirmed using SEM, XRD and TEM. Electrodes with bare PC and PC/CON was prepared and tested using a battery analyzer. The PC/CON electrode showed significantly higher specific capacity and better capacity retention up to forty cycles. The investigation shows the potential of using metal oxide nanoparticles on carbonaceous materials as an intriguing way of improving the performance of Li ion batteries.

6.2 High-performance Porous Carbon/CeO2 Nanoparticles Hybrid Super-capacitors for Energy Storage

Energy storage/harvesting research are indispensable in today's world which faces challenges such as environmental problems and the depletion of fossil fuels. Thus there is a need for better energy systems with enhanced performance from current available technology. Super capacitors which use hybrid carbon-metal oxide electrodes may provide a solution which results in enhanced energy and power density, cyclic stability and life. Here a method has been presented which uses a simple one-step low temperature hydrothermal process to fabricate PC-CON

electrodes. This hybrid electrode combination allows for the hybridization of the best attributes of each singular electrode material. SEM, TEM and HRTEM images confirmed the formation of crystalline nanoparticles in the hydrothermal reaction. Only porous carbon and CeO2 were found in the XRD analysis. Based on the electrochemical results, it is obvious that PC-CON hybrid electrodes have promising future for electrochemical energy storage. This simple method can be utilized for making high performance super-capacitor for next generation aerospace, automobile and electronic application.

6.3 Microwave Exfoliated Graphene Oxide/TiO_2 Nanowire Hybrid for High Performance Lithium Ion Battery

Energy storage devices, i.e., battery and super-capacitors, are the bases for green energy solutions. A simple method of graphene oxide exfoliation was utilized through microwave radiation and a low-temperature hydrothermal method was employed to synthesize MEGO-TON hybrid material for high performance LIB electrode. SEM image demonstrated that the porous structure was obtained after microwave treatment and nanowires are uniformly distributed on the exfoliated graphene oxide surface after thermal reduction. Highest 80% improvement of specific capacity was found from MEGO-TON hybrid electrode compared to the as purchased PC electrode material in terms of capacitance and cycle stability. The growth of nanowires has a positive synergistic effect that prevents graphene agglomeration and provides pathways for Li-ion insertion/extraction increasing electrode-electrolyte contact area. This simple method can be utilized in a larger scale for high-performance LIBs.

References

1. U.S. Energy Information Administration. Today in energy. n.d. 2015. <http://www.eia.gov/todayinenergy/images/2013.07.25/worldenergy.png >.

2. Wikipedia. Energy Consumption. n.d. 2015. <https://upload.wikimedia.org/wikipedia/commons/1/17/US_Energy_Consumption_by_Source_2013.png >.

3. Wikipedia. Energy Consumption. n.d. 2015. <https://upload.wikimedia.org/wikipedia/commons/b/b6/Total_World_Energy_Consumption_by_Source_2013.png >.

4. Geim, Andre Konstantin. "Graphene: status and prospects." science 324.5934 (2009): 1530-1534.

5. Singh, Virendra, et al. "Graphene based materials: past, present and future."Progress in Materials Science 56.8 (2011): 1178-1271.

6. Wajid, Ahmed S., et al. "Polymer-stabilized graphene dispersions at high concentrations in organic solvents for composite production." Carbon 50.2 (2012): 526-534.

7. Geim, Andre K., and Konstantin S. Novoselov. "The rise of graphene." Nature materials 6.3 (2007): 183-191.

8. Asbury Carbons. Asbury Carbons. 2013. 2015. <http://asbury.com/technical-presentations-papers/introduction-to-graphite/>.

9. Chemistry Land. Hybridization: Flexibility at its best. n.d. 2015. <http://www.chemistryland.com/CHM151S/09-CovalentBonds/Covalent.html>.

10. Chemistry. n.d. 2015. <http://bioserv.fiu.edu/~walterm/human_online/chemistry/chemistry1.htm >.

11. Choi, Wonbong, et al. "Synthesis of graphene and its applications: a review."Critical Reviews in Solid State and Materials Sciences 35.1 (2010).

12. Marcano, Daniela C., et al. "Improved synthesis of graphene oxide." ACS nano4.8 (2010): 4806-4814.

13. Wajid, Ahmed S., et al. "High-Performance Pristine Graphene/Epoxy Composites With Enhanced Mechanical and Electrical Properties."Macromolecular Materials and Engineering 298.3 (2013): 339-347.

14. Frackowiak, Elzbieta, and Francois Beguin. "Carbon materials for the electrochemical storage of energy in capacitors." Carbon 39.6 (2001): 937-950.

15. Namisnyk, Adam Marcus. A survey of electrochemical supercapacitor technology. Diss. University of Technology, Sydney, 2003.

16. Simon, Patrice, and A. F. Burke. "Nanostructured carbons: double-layer capacitance and more." The electrochemical society interface 17.1 (2008): 38.

17. Wikipedia. Supercapacitor. n.d. 2015. <https://en.wikipedia.org/wiki/Supercapacitor>.

18. Schneuwly, Adrian, and Roland Gallay. "Properties and applications of supercapacitors: From the state-of-the-art to future trends." Rossens, Switzerland (2000).

19. Stojek, Zbigniew. "The electrical double layer and its structure."Electroanalytical Methods. Springer Berlin Heidelberg, 2010. 3-9.

20. Grahame, David C. "The electrical double layer and the theory of electrocapillarity." Chemical reviews 41.3 (1947): 441-501.

21. Halper, Marin S., and James C. Ellenbogen. "Supercapacitors: A brief overview." The MITRE Corporation, McLean, Virginia, USA (2006): 1-34.

22. Srinivasan, Supramaniam. "Electrode/electrolyte interfaces: Structure and kinetics of charge transfer." Fuel Cells. Springer US, 2006. 27-92.

23. Namisnyk, Adam Marcus. A survey of electrochemical supercapacitor technology. Diss. University of Technology, Sydney, 2003.

24. Conway, B. E., and W. G. Pell. "Double-layer and pseudocapacitance types of electrochemical capacitors and their applications to the development of hybrid devices." Journal of Solid State Electrochemistry 7.9 (2003): 637-644.

25. Armand, Michel, and J-M. Tarascon. "Building better batteries." Nature451.7179 (2008): 652-657.

26. Tarascon, J-M., and Michel Armand. "Issues and challenges facing rechargeable lithium batteries." Nature 414.6861 (2001): 359-367.

27. Rajib, M., Shuvo, M. A. I., Karim, H., Delfin, D., Afrin, S., & Lin, Y., “Temperature influence on dielectric energy storage of nanocomposites.” Ceram. Int., 41(1), 1807-1813(2015)

28. Zhou, H., Zhu, S., Hibino, M., & Honma, I. “Electrochemical capacitance of self-ordered mesoporous carbon,” J. Power Sources, 122(2), 219-223(2003)

29. Mendoza, M., Rahaman Khan, M. A., Ishtiaque Shuvo, M. A., Guerrero, A., & Lin, Y., "Development of lead-free nanowire composites for energy storage applications," ISRN, (2012).

30. Futaba, Don N., et al. "Shape-engineerable and highly densely packed single-walled carbon nanotubes and their application as super-capacitor electrodes."Nature materials 5.12 (2006): 987-994.

31. Shuvo, M. A. I., Tseng, T. L. B., Khan, M. A. R., Karim, H., Morton, P., Delfin, D., & Lin, Y., "Nanowire modified carbon fibers for enhanced electrical energy storage," J. Appl. Phy., 114(10), 104306(2013)

32. Mohri, M., et al. "Rechargeable lithium battery based on pyrolytic carbon as a negative electrode." Journal of Power Sources 26.3 (1989): 545-551.

33. Shuvo, Mohammad Arif Ishtiaque, et al. "Investigation of modified graphene for energy storage applications." ACS applied materials & interfaces 5.16 (2013): 7881-7885.

34. Pang, Huan, and Changyun Chen. "Facile synthesis of cerium oxide nanostructures for rechargeable lithium battery electrode materials." RSC Advances 4.29 (2014): 14872-14878.

35. Liu, Wei, et al. "A facile hydrothermal synthesis of 3D flowerlike CeO 2 via a cerium oxalate precursor." Journal of Materials Chemistry A 1.23 (2013): 6942-6948.

36. Qi, Rui-Juan, et al. "Sonochemical synthesis of single-crystalline CeOHCO3 rods and their thermal conversion to CeO2 rods." Nanotechnology 16.11 (2005): 2502.

37. Liu, Mingxian, et al. "Development of MnO 2/porous carbon microspheres with a partially graphitic structure for high performance supercapacitor electrodes."Journal of Materials Chemistry A 2.8 (2014): 2555-2562.

38. Shuvo, Mohammad Arif Ishtiaque, et al. "Investigation of modified graphene for energy storage applications." ACS applied materials & interfaces 5.16 (2013): 7881-7885.

39. Wang, Donghai, et al. "Self-assembled TiO2–graphene hybrid nanostructures for enhanced Li-ion insertion." ACS nano 3.4 (2009): 907-914.

40. Rajib, Md, et al. "Temperature influence on dielectric energy storage of nanocomposites." Ceramics International 41.1 (2015): 1807-1813.

41. Mendoza, Miguel, et al. "Development of lead-free nanowire composites for energy storage applications." ISRN Nanomaterials 2012 (2012).

42. Shuvo, Mohammad Arif Ishtiaque, et al. "Nanowire modified carbon fibers for enhanced electrical energy storage." Journal of Applied Physics 114.10 (2013): 104306.

43. XianáGuo, Chun, and Chang MingáLi. "CeO 2 nanoparticles/graphene nanocomposite-based high performance supercapacitor." Dalton Transactions40.24 (2011): 6388-6391.

44. Padmanathan, N., and S. Selladurai. "Shape controlled synthesis of CeO2 nanostructures for high performance supercapacitor electrodes." RSC Adv.4.13 (2014): 6527-6534.

45. Zhi, Mingjia, et al. "Nanostructured carbon–metal oxide composite electrodes for supercapacitors: a review." Nanoscale 5.1 (2013): 72-88.

46. Shuvo, Mohammad Arif I., et al. "High-performance porous carbon/CeO2 nanoparticles hybrid super-capacitors for energy storage." SPIE Smart Structures and Materials+ Nondestructive Evaluation and Health Monitoring. International Society for Optics and Photonics, 2015.

47. Wang, Hailiang, et al. "Mn3O4− graphene hybrid as a high-capacity anode material for lithium ion batteries." Journal of the American Chemical Society132.40 (2010): 13978-13980.

48. Yoo, EunJoo, et al. "Large reversible Li storage of graphene nanosheet families for use in rechargeable lithium ion batteries." Nano letters 8.8 (2008): 2277-2282.

49. Li, Chengchao, et al. "Porous carbon nanofibers derived from conducting polymer: synthesis and application in lithium-ion batteries with high-rate capability." The Journal of Physical Chemistry C 113.30 (2009): 13438-13442.

50. Wu, Zhong-Shuai, et al. "Graphene anchored with Co3O4 nanoparticles as anode of lithium ion batteries with enhanced reversible capacity and cyclic performance." ACS nano 4.6 (2010): 3187-3194.

51. Ji, Liwen, and Xiangwu Zhang. "Fabrication of porous carbon nanofibers and their application as anode materials for rechargeable lithium-ion batteries."Nanotechnology 20.15 (2009): 155705.

52. Karim, Hasanul, et al. "Porous carbon/CeO2 composites for Li-ion battery application." SPIE Smart Structures and Materials+ Nondestructive Evaluation and Health Monitoring. International Society for Optics and Photonics, 2015.

53. Wu, Zhong-Shuai, et al. "Doped graphene sheets as anode materials with superhigh rate and large capacity for lithium ion batteries." ACS nano 5.7 (2011): 5463-5471.

54. Kim, Hyesun, and Jaephil Cho. "Superior lithium electroactive mesoporous Si@ Carbon core− shell nanowires for lithium battery anode material." Nano Letters8.11 (2008): 3688-3691.

55. Yang, Juan, et al. "A hierarchical porous carbon material for high power, lithium ion batteries." Electrochimica Acta 56.24 (2011): 8576-8581.

56. Armstrong, Graham, et al. "TiO2 (B) Nanowires as an Improved Anode Material for Lithium-Ion Batteries Containing LiFePO4 or LiNi0. 5Mn1. 5O4 Cathodes and a Polymer Electrolyte." Advanced Materials 18.19 (2006): 2597-2600.

57. Kavan, L., et al. "Nanocrystalline TiO2 (anatase) electrodes: surface morphology, adsorption, and electrochemical properties." Journal of the electrochemical society 143.2 (1996): 394-400.

58. Zukalova, Marketa, et al. "Pseudocapacitive lithium storage in TiO2 (B)."Chemistry of Materials 17.5 (2005): 1248-1255.

59. Zhu, Xianjun, et al. "Nanostructured reduced graphene oxide/Fe2O3 composite as a high-performance anode material for lithium ion batteries." Acs Nano 5.4 (2011): 3333-3338.

60. Hu, Y-S., et al. "Improved electrode performance of porous LiFePO4 using RuO2 as an oxidic nanoscale interconnect." Advanced Materials 19.15 (2007): 1963-1966.

61. Yoo, Eunjoo, and Haoshen Zhou. "Li− air rechargeable battery based on metal-free graphene nanosheet catalysts." ACS nano 5.4 (2011): 3020-3026.

62. Wang, Yan, et al. "Supercapacitor devices based on graphene materials." The Journal of Physical Chemistry C 113.30 (2009): 13103-13107.

63. Li, Changqing, et al. "Controllable preparation and properties of composite materials based on ceria nanoparticles and carbon nanotubes." Journal of Solid State Chemistry 181.10 (2008): 2620-2625.

64. Jian, Li, et al. "Review of electrochemical capacitors based on carbon nanotubes and graphene." Graphene 2012 (2012).

65. Liu, Hao, et al. "Highly ordered mesoporous NiO anode material for lithium ion batteries with an excellent electrochemical performance." Journal of Materials Chemistry 21.9 (2011): 3046-3052.

66. Chen, Ying-Chu, et al. "Highly flexible supercapacitors with manganese oxide nanosheet/carbon cloth electrode." Electrochimica Acta 56.20 (2011): 7124-7130.

67. Stoller, Meryl D., and Rodney S. Ruoff. "Best practice methods for determining an electrode material's performance for ultracapacitors." Energy & Environmental Science 3.9 (2010): 1294-1301.

68. Kumar, Akshay, Anuj R. Madaria, and Chongwu Zhou. "Growth of aligned single-crystalline rutile TiO2 nanowires on arbitrary substrates and their application in dye-sensitized solar cells." The Journal of Physical Chemistry C114.17 (2010): 7787-7792.

69. Yang, Ting, et al. "Cyanobacterium metallothionein decorated graphene oxide nanosheets for highly selective adsorption of ultra-trace cadmium." Journal of Materials Chemistry 22.41 (2012): 21909-21916.

70. Pang, Huan, and Changyun Chen. "Facile synthesis of cerium oxide nanostructures for rechargeable lithium battery electrode materials." RSC Advances 4.29 (2014): 14872-14878.

71. Cui, Li-Feng, et al. "Carbon− silicon core− shell nanowires as high capacity electrode for lithium ion batteries." Nano Letters 9.9 (2009): 3370-3374.

Vita

Gerardo Rodriguez Melo was born on the 21st of May in Monterrey, Mexico. He aspires for a career in industry as well as to get married and start a family. He graduated from Franklin High School in El Paso, Texas in 2008. Then, he graduated with a Bachelor's degree in Mechanical Engineering from the University of Texas at El Paso in 2013. Gerardo started his graduate degree in 2013 where he worked as a research assistant under the direction of Dr. Yirong Lin, a young and energetic professor with a lot of drive. Under Dr. Lin's caring tutelage and with the support of his wonderful and extremely gifted research group members, Gerardo was able grow in experience and skill, managing to contribute to the research being conducted and supporting several article publications and conference papers in which Gerardo took a part in. Overall, the environment and people that took part in Gerardo's life during his Master's coursework gave him a better perspective and relation with the engineering, scientific and even the professional world.

Permanent address: 4111 Westcity Ct. Apt. 105
El Paso, Texas, 79902

This thesis/dissertation was typed by Gerardo Rodriguez Melo.